Black Holes and Quantum Gravity at the LHC

Black Holes and Quantum Gravity at the LHC

Patrick Meade and Lisa Randall

Jefferson Physical Laboratory
Harvard University
Cambridge, MA 02138, USA

meade@physics.harvard.edu,randall@physics.harvard.edu

Abstract

We argue that the highly studied black hole signatures based on thermal multiparticle final states are very unlikely and only occur in a very limited parameter regime if at all. However, we show that if the higher-dimensional quantum gravity scale is low, it should be possible to study quantum gravity in the context of higher dimensions through detailed compositeness-type searches.

1 Introduction

One of the most exciting possibilities for the LHC is the discovery of small higher-dimensional [1] black holes that could be formed when two sufficiently energetic particles collide [2, 3, 4, 5]. Ideally, such black holes would decay isotropically to many energetic particles, in keeping with the prediction of thermal Hawking radiation [6]. However, over most of the viable parameter space, this expectation is not very realistic. Once inelasticity and black hole entropy are accounted for, it is clear that multiparticle final states are very suppressed, since only black holes produced well above threshold have sufficient entropy. The falling parton distribution functions(PDFs) more than compensate for the rise in black hole production with energy so most strong gravity events will occur at the lowest possible energy scale.

Nonetheless, all is not lost. Even when the energy is too low to produce truly thermal black holes, which require sufficiently high entropy and energy, we would nevertheless expect signs of quantum gravity if higher dimensional gravity gets strong at a scale not too far above a TeV. Strong gravity is likely to result in more spherical final states, even for those final states with low multiplicity, which would therefore be measured as much more transverse than background. As we will show, over most regions of expected parameter space for higher dimensional models, we expect a significant change in the rate of highly transverse two particle final states to occur at the quantum gravity scale, both jet-like and leptonic, although the latter rate which is smaller spans a smaller region of parameter space. Strong gravity should be testable through standard compositeness tests.

In fact, the threshold for a rise in the $2 \to 2$ scattering cross section is almost inevitably lower than the black hole production threshold. Though not necessarily a true thermal black hole, these final states, if they occur, will nonetheless tell us about quantum gravity. In fact, in the thermal regime, black holes wouldn't give us *any* insight into quantum gravity (except to confirm existing theoretical predictions). In the region at or below the true thermal black hole threshold, assuming strong gravity effects don't turn on or off suddenly at the black hole scale, we could in principle learn a lot by studying the two particle final states, in particular the angular distribution and the energy dependence of the angular distribution which would truly be quantum gravity results, not interpretable in terms of a classical calculation.

Furthermore we will see that there is sufficient information to distinguish not only black hole type effects, but different forms of string amplitudes. This can in principle probe the effects of curvature or non-string objects in the theory as well. Moreover, we don't expect only strong gravity effects if higher dimensional theories are right. We should in that case find indications of KK final states at lower energy. In that case there would be indications whether composite-type effects might be associated with quantum gravity to help us disentangle it from other strongly interacting physics. In what follows, we will see other possible distinctive features of gravitational physics that might help distinguish among possibilities. Thus what we are saying is that even existing compositeness searches don't just tell about strong gauge dynamics-they could in principle tell us about gravity as well. We show how we can hope to learn about black hole production and quantum gravity by studying the energy dependence of the high p_T dijet or leptonic cross section. We consider the implications of a rise or fall in the cross section and what the energy dependence might teach us about quantum gravity.

We stress that although the two particle final state signal is unlikely to probe thermal black holes in the accessible energy range, it is of great interest as a way of probing quantum gravity. The rate as a function of energy as well as the angular distribution can differ significantly in various scenarios of quantum gravity. Furthermore in almost any scenario we expect the two particle final state to demonstrate effects of quantum gravity well before the proposed multiparticle final states characteristic of thermal black holes. Furthermore whereas we know the predictions for the semiclassical regime, independent of the particular theory of quantum gravity, the threshold regime can potentially distinguish among them.

Others have considered the effects of specific gravitational effects on higher-dimensional operators and how they can be constrained by existing searches. Ref. [7] considered a dimension-8 operator, Ref. [8] considered graviton loops generating a dimension-6 operator, Ref. [9, 10] considered string-generated dimension-8 operators and string resonances, Ref. [11] considered dimension-6 operators from string theory. Our point is to view compositeness searches more generally and to learn how to distinguish among the possibilities rather than to constrain the scale of any one particular model. Furthermore we emphasize that the gap between the quantum gravity scale and the true black hole threshold should be a good source of deviations in 2→2 scattering and probably yields a much better reach and more insight than multiparticle searches.

2 Black Hole Production and Decay

The large black hole cross section estimate stems from the classical cross section that is proportional to the geometrical area set by the Schwarzschild radius r_S:

$$\sigma(E) \sim \pi r_S(E)^2. \tag{2.1}$$

This geometrical cross section implies

$$\sigma(E) \sim \frac{1}{M^2}\left(\frac{E}{M}\right)^{\alpha} \tag{2.2}$$

where M is the effective scale of quantum gravity and $\alpha \leq 1$ for higher-dimensional black holes. Thus for instance at the LHC one might expect a parton-parton cross section of size at least $\sim \frac{1}{M^2}$, which for $M \sim 1$ TeV corresponds to an enormous rate of approximately 100 pb which for 100 fb^{-1} luminosity would yield ten million events. The basic reason why this cross section is so large compared to the production of a particle with TeV mass in a typical beyond the SM theory is the lack of any small couplings, such as gauge couplings in the cross section and the absence of phase space suppression factors. However, this estimate ignores several major considerations and uncertainties in the black hole production[3, 2] and decay cross sections that we discuss in the rest of this section.

There have been relatively few studies of the phenomenological consequences of RS black holes, and thus in addition to elaborating the points above we will also expand further upon this case throughout the paper and in Appendix A. Landsberg [12] discussed RS black

hole signatures, but used more optimistic assumptions for parameter space than are now experimentally allowed and neglected the inelasticity that we will soon discuss. Ref. [13] considered black holes that might arise in warped five-dimensional space in the context of cosmic ray searches. For further references see Appendix A. We will see in Appendix A that in the energy range between $\tilde{M}$ and $(M/k)^2\tilde{M}$, where M is the five dimensional Planck scale($\tilde{M}$ is M reduced by a warp factor) and k is related to the AdS curvature, we expect to a good approximation conventional five-dimensional black holes. Of course, in the RS case where approximately flat space black holes occur only over a limited energy range, we would need M/k large enough to permit high entropy black holes.

2.1 Criteria for Black Holes

The production cross section in (2.1) depends only on the mass scales involved and thus appears to be a very simple quantity to understand. Unfortunately however there are ambiguities associated with both of the two scales in the problem, M and M_{BH}. Since one makes rough estimates assuming black holes start forming at a scale M, and due to the falling PDFs[(1)] the rate changes dramatically depending on the scale at which black holes start to form, it is critical to keep track of the different conventions for the Planck scale and the relationships among them so that we can unambiguously compare rate predictions. See Figure 1 to see the different relative contributions to $2 \to 2$ scattering from the pdfs. These will be helpful in understanding results throughout the paper.

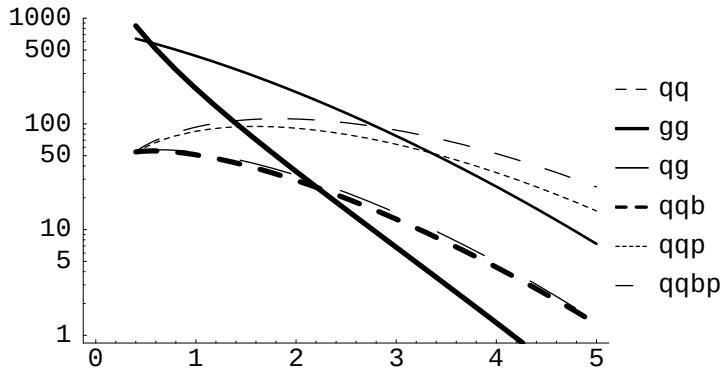

Figure 1: Arbitrarily normalized parton-parton luminosity plot as a function of $\sqrt{\hat{s}}$ to show the relative contributions of initial state partons.

Different authors have used different conventions for normalizing the Planck scale. We

[(1)]The effective scaling of the PDFs can be summarized in terms of a parton luminosity. See for instance Figure 69 of [14]. The drop in the parton luminosity at the LHC depends on the mass range of interest, for instance for qq and $\sqrt{\hat{s}} \sim 1 - 2$ TeV the luminosity drops off approximately as $\sim 1/\hat{s}$ while for higher invariant mass it can drop off as $\sim 1/\hat{s}^4$.

define G_D with the Myers-Perry convention [15]

$$\frac{1}{16\pi G_D}\int d^{D+1}x\sqrt{g}R \tag{2.3}$$

and define $\mathcal{L}_N$ as the normalization of the Einstein-Hilbert action for which (2.3) gives $1/16\pi G_D$. In the case of n extra dimensions, the PDG convention [17] is $\mathcal{L}_N = M_D^{n+2}/2(2\pi)^n$ whereas the early analysis of Dimopoulos and Landsberg [2] used $M_P^{n+2}/16\pi$. Although neither analysis was done for case of one extra dimension due to the constraints on $n = 1$ ADD type set ups [16], there is a range of mass scales for which approximate five-dimensional flat space black holes would be the most appropriate description for RS models (see Appendix A). To illustrate the convention dependencies we give their formulae for $n = 1$ so as to compare to RS, in which case their formulae reduce to $\tilde{M}_P^3/16\pi$ and $\tilde{M}_D^3/4\pi$, which should be compared to $\tilde{M}^3/2$, which is the RS convention, where the tilde indicates the warped version of the various Planck scales. Although just conventions, it is important to bear these conventions in mind when interpreting results.

The Schwarzschild radius of the black hole given in [15] for the $(4+n)$-dimensional case is

$$r_S = \left(\frac{M_{BH}\Gamma\left(\frac{n+3}{2}\right)}{\mathcal{L}_N(n+2)2\pi^{\frac{n+3}{2}}}\right)^{\frac{1}{n+1}} \tag{2.4}$$

where the scale is understood to be appropriately warped in the RS case (for details see the Appendix), which reduces to

$$\left(\frac{M_{BH}}{\mathcal{L}_N 6\pi^2}\right)^{1/2} \tag{2.5}$$

for the case of $n = 1$. Using the RS normalization of the action we find that the Schwarzschild radius in RS1 is given by

$$r_S = \left(\frac{M_{BH}}{\tilde{M}^3 3\pi^2}\right)^{1/2}. \tag{2.6}$$

For the case of one extra dimensions, the DL and PDG conventions would give

$$r_S^{DL} = \left(\frac{8M_{BH}}{M_P^3 3\pi}\right)^{1/2} \quad r_S^{pdg} = \left(\frac{2M_{BH}}{M_D^3 3\pi}\right)^{1/2} \tag{2.7}$$

where M_P and M_D are the higher-dimensional Planck scales in the two cases.

Although just a convention, the numerical relationships mean that if we take $r_S \sim 1/M$ as the threshold for black hole production, comparing the two formulations of the Schwarzschild radius in the case of [2] we would find that black holes would be produced at energies $\sim M_P$, while in [18] black holes would be produced at a scale of $\sim 4^{1/3} \sim 1.6M_D$ while the convention would yield $(8\pi)^{1/3}\tilde{M} \sim 2.9\tilde{M}$. These conventions are clearly significant in interpreting the meaning of the black hole energy reach for the LHC and comparing to experimental constraints. Of course the physical answers are not convention dependent.

When we compare the scales relative to threshold production to the current experimental bounds on KK masses, the convention dependence drops out.

The real question is the black hole threshold where black holes start to form. Of course at center of mass energies much greater than the higher-dimensional Planck scale, M, we know black holes will be produced. However, the precise threshold is ambiguous. M is after all convention dependent. Though we will assume $E > M$ is necessary, it is clearly not sufficient.

Since we don't know the precise threshold for a truly thermal black hole, it is useful to define a parameter x_{min} that tells how far above the relevant Planck scale the semiclassical prediction applies [3]. This could be defined relative to an arbitrary threshold mass or relative to the convention-dependent Planck scale. We will use the latter with the understanding that x_{min} is unknown either way and is simply a parameter. In our analysis we will give results as a function of M and x_{min}. We consider criteria for x_{min} below. Note that we would want x_{min} for RS to be less than $(M/k)^2$ where the curvature becomes relevant as outlined in Appendix A.

Keep in mind that in addition to significantly reducing the black hole production cross section, the existence of a nontrivial x_{min} obscures our ability to extract fundamental parameters from the black hole cross section. The overall cross section depends very strongly on x_{min} since as we have already noted, the rapid fall-off of the PDFs makes us very sensitive to the mass threshold where black hole production can begin. This means that any potential bounds from an LHC experiment on black hole production rates is only indirectly related to the fundamental scale of quantum gravity. For instance if one finds an excess of events attributed to black hole it is unclear how to translate back to the scale M involved if one is only looking on the tail of a distribution.

Without knowing more about the threshold behavior of black hole production, the dependence of the cross section on the fundamental Planck scale is insufficient to extract that parameter, which can be mimicked by an alternate choice of x_{min}. In principle, the energy-dependence of the cross section can be useful in extracting the number of dimensions (if we know the PDFs sufficiently accurately), although in practice this will be very challenging. In any case, this slope won't determine the higher-dimensional Planck scale. In principle, the differential cross section can be used to extract the Planck scale since, once it has turned on, the cross section depends on black hole mass (not x_{min}). But without the energy-dependent inelasticity factor (see below) this will be impossible. Furthermore, uncertainties in PDFs and the experimental determination of energy scale will also make this unlikely.

2.2 Thermality

Although difficult to quantify precisely, we now consider several possible criteria for the formation of a truly thermal black hole. Though not sufficient, we expect these to be some minimum necessary criteria that will give some sense of what x_{min} should be.

The first criterion one might apply is that the Compton wavelength of the colliding particle of energy $E/2$ lies within the Schwarzschild radius for a black hole of given energy E. If we define the threshold as the point where a wave with wavelength $4\pi/E$ lies within

the Schwarzschild radius for a black hole of mass E, we find for ADD $n = 6$ black holes this yields $x_{min} > 4.1$ (in the M_D convention). Had we simply required $r_S > 1/E$, we would have the weaker criterion $x_{min} > 0.44$. In the RS case, we find with the stronger criterion that $x > 16$, whereas with the weaker criterion it should be greater than about 3. We see that this criterion in and of itself if fairly strong, and already will make black hole production very small or *nonexistent* given LHC parameters.

Even so, the above criterion is not necessarily sufficient to guarantee a black hole since we don't expect the semiclassical formula to apply at the threshold determined above. For a black hole to be truly thermal, we expect higher entropy is required and therefore the threshold will be above the energy we just considered. There are several additional criteria that we would want to be satisfied, all roughly amounting to the fact that the black hole should be sizable enough that the entropy is large. Although for sufficiently large black holes, any criteria of the sort below will be amply satisfied, as we have emphasized, the falling PDFs tell us production is dominated by near-threshold objects.

For the criteria below, the following formula will prove useful. For n extra dimensions we have

$$r_S = \frac{1+n}{4\pi T} = \frac{k(n)}{M_D}\left(\frac{M_{BH}}{M_D}\right)^{\frac{1}{1+n}}, \tag{2.8}$$

where

$$k(n) = \left(2^n \pi^{\frac{n-3}{2}} \frac{\Gamma\left(\frac{n+3}{2}\right)}{2+n}\right)^{\frac{1}{1+n}} \tag{2.9}$$

$$S = \frac{1+n}{2+n}\frac{M_{BH}}{T_{BH}} \tag{2.10}$$

It is also useful to consider the average number of particles assuming the decay is mostly on the brane [19]. The prediction for black hole decays in experiments have been approached in a couple of ways, including treating the decay as instantaneous[2], evolving with mass[18, 20], and sometimes including the appropriate grey body factors for the extra-dimensional black holes as well. These distinctions have an order one impact on the average number of particles comparing for instance to an instantaneous decay calculation with

$$\langle N \rangle = \left(\frac{2\sqrt{\pi}}{n+1}\right)\left(\frac{M_{BH}}{M_P}\right)^{(n+2)/(n+1)}\left(\frac{8\Gamma((n+3)/2)}{2+n}\right)^{1/(n+1)} \tag{2.11}$$

compared to one that evolved the black hole with mass and included greybody factors

$$\langle N \rangle = \rho S_0 = \rho\left(\frac{4\pi k(n)}{2+n}\right)^{(n+2)/(n+1)}\left(\frac{M_{BH}}{M_D}\right)^{(n+2)/(n+1)}. \tag{2.12}$$

Allowing for the difference in the definitions of the Planck scales, the instantaneous decay gives particle number a factor of 1.44 times that calculated by decaying over time. The mass scaling is in accordance with the mass-dependence of the entropy.

For the specific cases we will be interested we list the average number of particles emitted for ADD $n = 6$

$$\langle N \rangle \sim \frac{4\pi\rho k(6)}{8} \left(\frac{M_{BH}}{M_D}\right)^{\frac{8}{7}} \tag{2.13}$$

with

$$\rho = \frac{\sum c_i g_i \Gamma_i \zeta(3)\Gamma(3)}{\sum c_i f_i \Phi_i \zeta(4)\Gamma(4)} \tag{2.14}$$

which defines a ratio of multiplicities and greybody factors defined in [18]. For RS $n = 1$[(2)] we find

$$\langle N \rangle \sim \frac{4\rho}{3\sqrt{3}} \left(\frac{M_{BH}}{\tilde{M}}\right)^{\frac{3}{2}} \tag{2.15}$$

Notice that $\langle N \rangle = \rho S$.

In what follows below, we will use the grey-body corrected time-dependent decay estimate. Of course, near threshold, all these formulae are unreliable but give an idea of what one might expect.

- Preskill et al [21] give the criterion $|\partial T/\partial M| << 1$, which is equivalent to the change in Hawking temperature per particle emission should be small. This condition is equivalent to the entropy (2.10) being large. More specifically, $\partial T/\partial M \sim 1/((n+2)S)$. The improvement of this bound scales as $x_{min}^{\frac{2+n}{1+n}}$. This is not as strong a constraint as the other criteria we give below, for RS and ADD the constraint is satisfied already in both cases for $x_{min} = 1$

- We would also want the energy of any individual degree of freedom in a thermal bath to be much less than the black hole mass. This gives the criterion $(n + 3)T < M$ or equivalently $dM/dN << M$–that is, any one individual degree of freedom should not carry a significant fraction of the energy. This particular criterion is satisfied in ADD and RS for $x_{min} \gtrsim 2$. This condition is slightly subtle in the case when brane black hole decays are allowed, since the energy per degree of freedom for modes on the brane is reduced by roughly a factor of $3/(3 + n)$ since brane modes can oscillate only along the brane directions.

  You can also see this directly from the formulae for the rate of change of energy and number of particles when decaying into thermal d-dimensional states. In the former case, the decay rate is determined by $\int d^d k f(E)E$, whereas in the latter case it is determined by $\int d^d k f(E)$, where $f(E)$ is the Boltzmann factor. The resulting ratio whose inverse determines particle number is proportional to $d\xi(d + 1)/\xi(d)$, which is approximately d. That is, for decays into more dimensions (fixing T), we have fewer particles since each particle carries more energy. Even if the bulk modes don't dominate the decay, we would still not want any single bulk mode to carry a significant fraction of

[(2)] We approximate the greybody factor for $n = 1$ as the same as that for $n = 6$

the black hole energy if we are to interpret the decaying object as a higher-dimensional black hole.

This is a stricter criterion than above. We find one bulk degree of freedom carries almost all the energy when $M_{BH} \sim 3\tilde{M}$ in the case of RS, and slightly exceeds it in the case of ADD $M_{BH} \sim 2M_D(n=6)$. Clearly we would want $M_{BH} > M$ in both cases as the bound improves as $x_{min}^{(2+n)/(1+n)}$, again scaling as the entropy.

Of course we should keep in mind this is the criterion for *one* degree of freedom in the bulk to carry all the mass. Clearly for a thermal black hole, we would want many particles carrying the energy, so the bound would be much stronger. For example, the maximum experimental reach on x_{min} for ADD $n = 6$ is about 6, which would correspond to only 3 bulk particles! For RS, the maximum x_{min} is about 10, corresponding to at most about 5 or 6 particles sharing the energy, which also seems inadequate for a truly thermal state.

- We want the black hole lifetime to be bigger than $1/M$, so that the black hole appears as a resonance [3]. This criterion scales roughly as the number of degrees of freedom modified by grey-body factors. This is borderline for $n = 6$ and reasonably well satisfied for $n = 1$. For completeness we give the formula for the lifetime in ADD:

$$\tau = \frac{(4\pi)^4 k(n)^2 M_D^{\frac{-2(2+n)}{1+n}} M_{BH}^{\frac{3+n}{1+n}}}{\alpha(1+n)^3(3+n)} \tag{2.16}$$

$$\alpha = \frac{1}{2\pi}\left(\sum c_i f_i \Phi_i\right)\zeta(4)\Gamma(4) \tag{2.17}$$

where the factors in α are defined in [18], and correspond to multiplicities and greybody factors. For the specific case of $n = 6$ we find

$$\tau = .7\frac{x_{min}^{9/7}}{M_D}. \tag{2.18}$$

In RS we can find $\langle N \rangle$ from (2.16) by substituting $n = 1$, and replacing M_D with $\tilde{M}$ and $k(1)$ with $1/3\pi^2$ to account for the RS normalization. The result of this is that in RS the lifetime is given by

$$\tau = .38\frac{x_{min}^2}{\tilde{M}}. \tag{2.19}$$

Using these criteria we find that in ADD the criteria is satisfied for $x_{min} \sim 1.3$ and in RS for $x_{min} \sim 1.6$.

- A sometimes stricter criterion in the case of black holes that can decay on the brane is that the lifetime should exceed the black hole radius, so that the black hole can reequilibrate as the black hole decays primarily along the brane. This requires in the ADD case that $x \gtrsim 3$ while for RS the constraint is satisfied for any x_{min}.

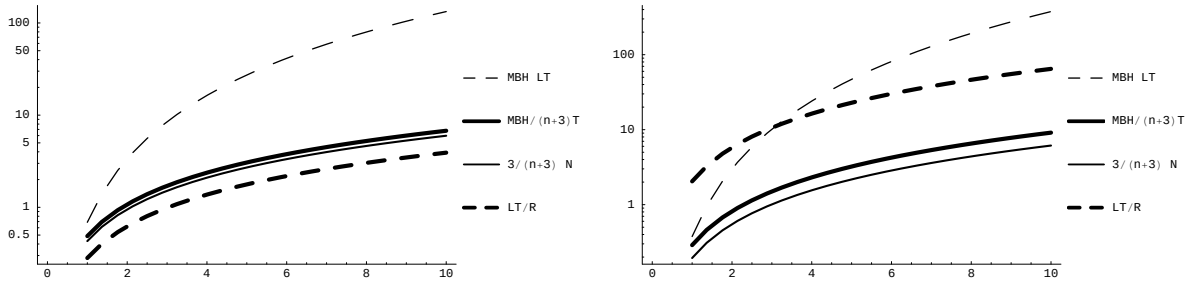

Figure 2: Possible criteria for x_{min} plotted as a function of x_{min}. ADD with n=6 is plotted on the left and RS is plotted on the right.

- The black hole's mass should be large compared to the 3-brane tension. We leave this criterion open since it is highly model-dependent.

The strongest criteria are plotted in Figure 2 as a function of x_{min} (with the exception of Schwarschild vs. Compton wavelength which would just be a vertical line) where the ratios are chosen such that every curve plotted should be greater than one if the criteria is satisfied. These criteria highlight the uncertainty in defining a precise threshold, and also indicate the blackhole threshold might be well above the putative Planck scale. We stress here that even though the various criteria might be satisfied for $x_{min} \gtrsim 3$ or 4 (except for the wavelength criterion), all these criteria are should really be held to being $\gg 1$ not just ~ 1 in which case x_{min} should be much larger in principle. They also show that the values of x_{min} that were used in previous analyses [3, 18] might be too low to trust to be in the thermal regime (and of course brings into question those analyses that neglected x_{min} entirely). As we will see however, higher values of x_{min} yield too low a production rate to appear at the LHC.

2.3 Inelasticity

In addition to the thermality criteria above that raise the black hole energy threshold, another critical effect is energy loss of the colliding partons before their energy is trapped behind a black hole horizon. One of the most important effects is to understand exactly how much energy of the initial parton parton system ends up going into the mass of the intermediate black hole. We can define an inelasticity parameter as in [18] $y \equiv M_{BH}/\sqrt{\hat{s}}$ which when less than 1 requires probing the PDFs at larger x and thus reducing the cross section possibly by many orders of magnitude compared to initial estimates[(3)].

The program of calculating this inelasticity goes back to unpublished work of Penrose and the work of D'eath and Payne [22, 23], who examined in four dimensions and zero

[(3)]There are other effects that modify the cross section, i.e. the maximum impact parameter that can still create a black hole in comparison to the Schwarzschild radius and $\mathcal{O}(1)$ factors in front of the putative cross section $\sigma \approx \pi r_S^2$ however for the LHC these effects are not nearly as crucial as the actual mass scale that defines the black hole production.

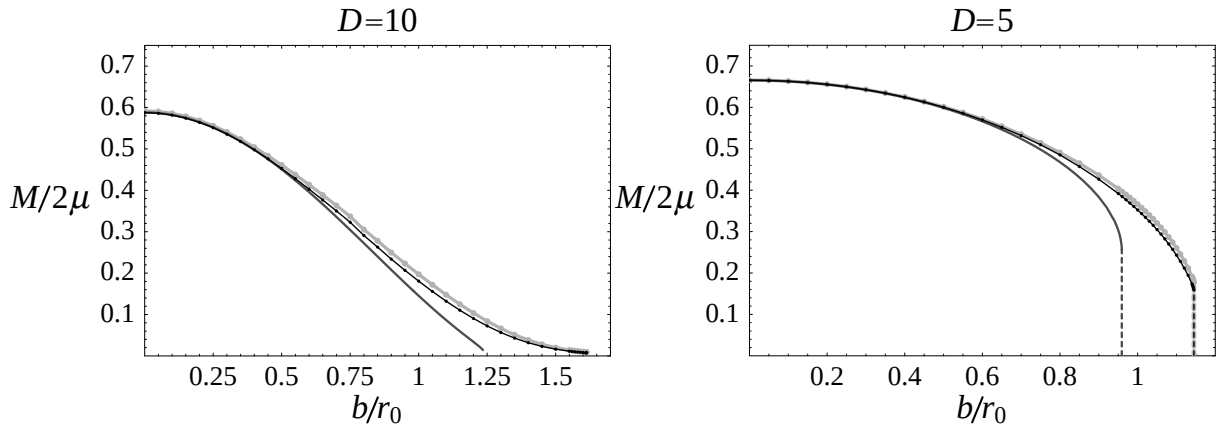

Figure 3: From Fig.10 of [26]. The ratio of the mass of the putative black hole compared to the initial energy of the collision is plotted as a function of the impact parameter divided by a unit r_0 that approximates the Schwarzschild radius if all the energy of the initial collision were to end up as a black hole. The lowest curve represents the calculation of [26], and previous estimates from [24, 25] are also included.

impact parameter, the fraction of energy emitted in gravitational waves when colliding to Aichelburg-Sexl shock waves representing two highly boosted massless particles. This work was extended to extra dimensions and non-zero impact parameters by the seminal work of Eardley and Giddings [24] and then further refined by [25, 26]. In Figure 3 we present the relevant results of [26], for the ratio of the mass trapped in the apparent horizon compared to initial energy as a function of the impact parameter for a 10 dimensional black hole (hereafter referred to as ADD) and 5 dimensional black hole (hereafter referred to as RS) which are relevant for our discussion.

As one can see from Figure 3 the largest energy fraction entering the black hole for both ADD and RS is $\mathcal{O}(.6)$ occurring for zero impact parameter. However they have different functional dependencies with respect to the impact parameter, and the ADD fraction goes down to $y \approx 0$ while RS goes to about $y \approx .2$ at the largest possible impact parameters where an apparent horizon still forms. These estimates are interpreted as lower bounds on the inelasticity but we stress that they are also calculated classically and for energies that are approaching the Planck scale it is not obvious how this will be modified.

To quantitatively include this inelasticity, we need to include the impact parameter dependent effect of inelasticity in calculating the black hole production cross section. Implicitly when calculating the cross section of a proton proton event we have summed over the possible impact parameter already when using the parton parton cross section

$$\sigma(pp \to X) = \sum_{i,j} \int dx_1 dx_2 f_i(x_1) f_j(x_2) \sigma(ij \to X). \tag{2.20}$$

To include the effects of inelasticity we adopt the impact parameter weighted average of the

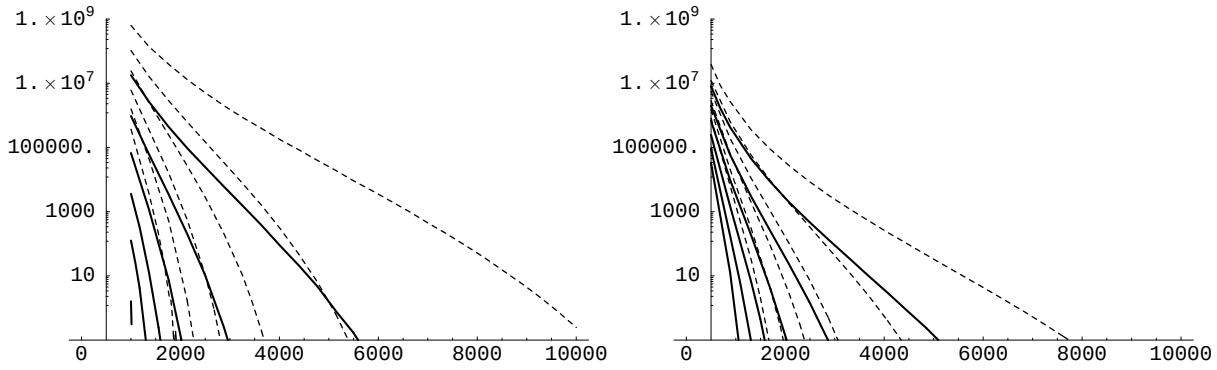

Figure 4: Total black hole cross section in femtobarns, including(solid curves) and not including(dashed) inelasticity as a function of M_D for ADD with $n = 6$ and $\tilde{M}$ for RS1. The different curves from highest to lowest correspond to $x_{min} = 1 - 6$.

inelasticity used in [18]

$$\sigma(pp \to BH) \equiv \sum_{i,j} \int_0^1 2zdz \int_{\frac{(x_{min}M_D)^2}{y(z)^2 s}}^1 du \int_u^1 \frac{dv}{v} f_i(v,Q) f_j(u/v,Q) \sigma_{i,j\to BH}(M_{BH} = us), \tag{2.21}$$

with $z = b/b_{max}$. The function $y(z)$ is given in our case by the results of [26], as shown in Figure 3. This weighting of the impact parameter obviously shows a difference between the RS and ADD cases, because in 10 dimensions the inelasticity parameter is smaller at order one impact parameters, meaning relatively higher energy will be needed to make a black hole. The total black hole cross section with and without inelasticity for both ADD and RS is shown in Figure 4. As demonstrated in Figure 4 the inclusion of inelasticity can reduce the total cross section by several orders of magnitude, which is consistent with the results of [18] who used [25] to define their inelasticity. It is interesting to note that these effects are more important for ADD than RS in terms of reduction of total cross section, as it is interesting that the inelasticity is higher for lower dimensions. While the rates presented in Figure 4 for the inclusion of inelasticity are taken as a lower bound for the black hole cross section, one should keep in mind that x_{min} lower than the criteria presented in Section 2.1 have been plotted and it is unclear what the "effective" inelasticity will be when quantum gravity effects are taken into account.

3 Black Hole Decays

In the previous sections we have argued that it is unlikely that the LHC will produce thermal black holes, since the thermality criteria require a black hole threshold above the putative higher-dimensional Planck scale and furthermore energy is lost through initial radiation. In this section we go a step further and argue that even if black holes were produced, they are

rarely if ever in a regime where they will produce the "fireball" explosions consisting of a high multiplicity isotropic distribution of particles that are the most highly emphasized [2, 3] black hole signature and possibly even revealing the negative specific heat that characterizes black holes.

Since this signature relies on high multiplicity events, it is worth checking over what parameter range one expects to find high multiplicities. Although not necessarily reliable for low multiplicities, we quantify this consideration by exploring the average number of particles assuming standard classical black holes with a thermal distribution of final state particles obeying Poisson statistics[18, 27] to determine the fluctuation about this mean value. The point is to show the relative merits of low and high multiplicity states. We use as a target "high multiplicity" six or more particles. Although far from a fireball, we are trying to allow the most optimistic assumption for a multiparticle state. We compare this reach to two body final states in the figures below.

In Figure 5 we plot the cross sections with and without inelasticity for both 6 or more particles(multiparticle) and 2 particles. To summarize and better demonstrate the relative potential strengths of multiparticle vs. two particle final states we plot in Figure 6 the region in parameter space for the multiparticle and 2 particle final states with a .1 fb cross section.

We see that the "reach"[(4)] of two particle final states is in all cases at least as good as the multiparticle final state. Therefore a study of low multiplicity final states might explore black hole-like objects even when x_{min} is not high enough to guarantee a thermal final state or a black hole.

To be as optimistic as possible, we also checked for the maximum number of particles assuming a .1 fb cross section according to a Poisson distribution for a given $\tilde{M}[M_D]$ where we looked for the maximum number of particles with that cross section. The maximum particle number in the RS case with a .1 fb cross section was on the order of 20 for $\tilde{M} = 500$ GeV and is about 9 for $\tilde{M} = 1$ TeV , and is only 6 for $\tilde{M}$ of 1.5 TeV. The maximum particle number in the ADD case for $M_D = 900$ GeV was about 20, for 1.4 TeV was about 14, and for 1.9 TeV was about 10. Although the later case might sound adequate, it should be kept in mind that this number depends on decays onto the brane. If we asked about the distribution of energy among thermal bulk particles, that is how many bulk particles would we expect for this sized black hole, the answer would be divided by 3. And this was for the best possible cases. So the black hole signature is not likely to be an isotropic burst of a large number of particles. Instead we expect low multiplicity final states to dominate.

Given the relative weakness of the muliparticle final states the likely black hole signature will not be an isotropic burst of a large number of particles. Instead we expect low multiplicity final states to dominate. We consider the consequences of this conclusion in the next section.

[(4)]Here we are defining reach as just a possible observation of signal assuming the background is non-existent. This is not meant to be a statistically significant reach; nevertheless it gives one the potential reach if backgrounds are under control. In the next section for the two particle states we will show backgrounds in the 2 particle state.

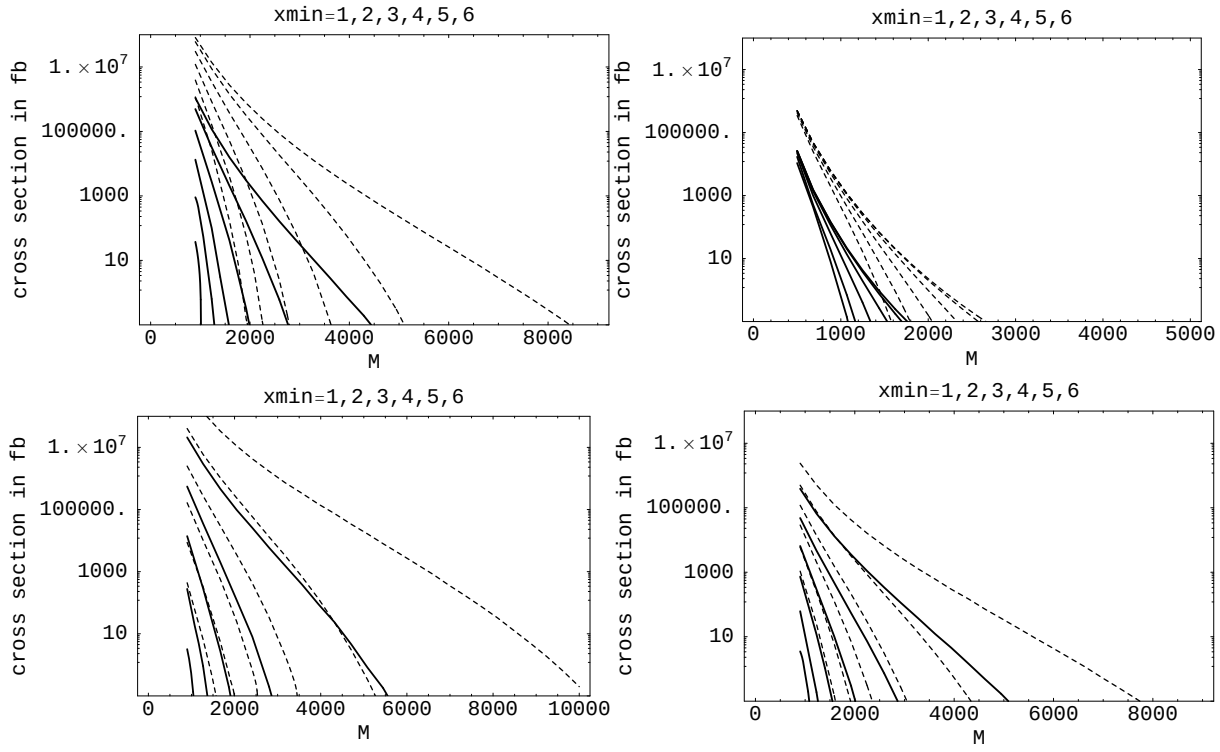

Figure 5: In the upper plots curves of total cross section for having 6 or more particles, including(solid curves) and not including(dashed) inelasticity as a function of M_D for ADD with $n = 6$ and $\tilde{M}$ for RS1. The different curves from highest to lowest correspond to $x_{min} = 1 - 6$. In the lower plots the same curves are plotted for having 2 particles instead of 6 or more.

4 Two Body Final States

Examining the formulae for the average number of particles emitted in the decays (2.13) and (2.14), we see that for RS only for $M_{BH} > 4\tilde{M}$ is the average number of particles emitted greater than 2, and for ADD you need $M_{BH} > 1.5M_D$. Clearly for x_{min} satisfying the criteria we've listed this is not a problem. But it makes manifest that for low x_{min} our "black holes" decay into only a small number of particles. However, even if the decay is not a true thermal black hole, some interesting new signature is likely to appear and could be a valuable indicator of strong gravity effects-one whose reach in almost all cases is comparable to or exceeding the reach of the multiparticle final states.

We now consider the implications of black holes, or other quantum gravity effects, for 2→2 scattering processes. Whether or not true black holes appear at center of mass energies of order the Planck mass, we expect that true or virtual black holes or simply strong gravity effects will lead to an increase in the 2→2 production cross section as we approach the Planck scale, as can be seen from the large cross sections in the previous section. Later on when

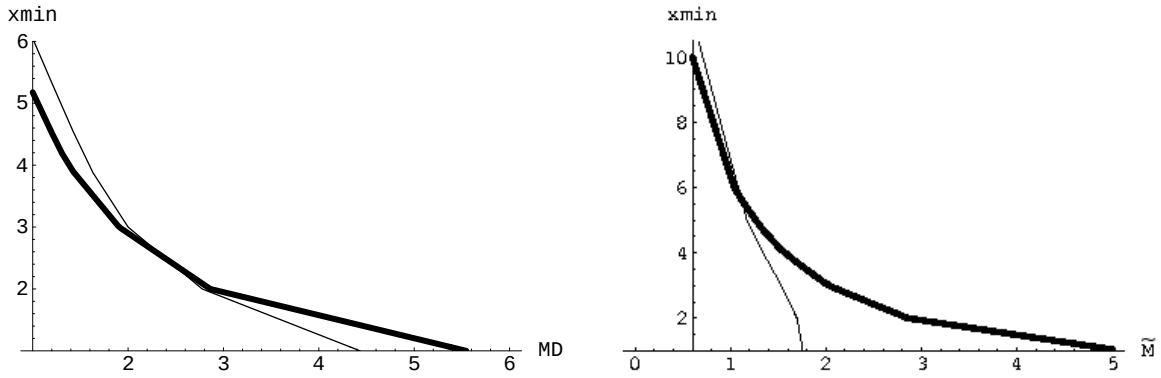

Figure 6: Curves of constant .1 femtobarn cross section including the effects of inelasticity and a probability for getting either 2 particles(thicker curve) or greater than 6 particles(thin curve). In the left hand panel the curves are for ADD with 6 extra dimensions and are plotted as a function of $x_{min} \equiv M_{BH}/M_D$ and M_D. In the right hand panel the curves are for RS1 as a function of $x_{min} \equiv M_{BH}/\tilde{M}$ and $\tilde{M}$.

we include backgrounds this increase will become even more manifest. In practice, because the calculation is inherently nonperturbative in this regime, we cannot precisely calculate the scattering. However, by considering a few examples we show that under reasonable assumptions we can gain insight into quantum gravity by studying these processes.

In principle exception to enhanced two-body production might be weakly coupled string theory. But in this case we would see the string states or other effects (see below) well before the black hole scale, which in any case would be out of reach (since it is of order M_S/g_s^2 [28]).

So rather than explore only the tail of black hole distributions where multiparticle states could dominate, we examine the Planckian "black holes" (by which we mean any quantum gravity effect or resonance) where $M_{BH} \sim M$. Given the PDF fall offs at the LHC and the flux limitation of UHECR experiments black holes will be dominantly produced at the lowest mass available to them in any foreseeable experimental setting that they could be potentially produced in. Taking into account inelasticity amongst other effects we don't expect high mass black holes, and one really needs to explore as low of mass "black holes" as possible within the context of the most quantitative statements that can be made.

Furthermore, we have seen by considering the maximum particle number that even under the most optimistic assumptions on scales and threshold, we are unlikely to create truly thermal high multiplicity black holes but instead low multiplicity states.

The most dramatic two body final state signature one might hope to find would be one that violates global quantum numbers, such as μ,e. However, since this physics occurs at the TeV scale, there are already strong constraints since turning around such a process would presumably permit flavor-changing lepton decays for example. This might occur through virtual black hole exchange or directly through the dangerous TeV-scale physics. The latter could be suppressed if there are effectively large anomalous dimensions—that is the operator turns on only at high energies. The former could be suppressed since we don't understand

virtual black holes. But we conservatively assume that there is either separation of particles in the higher dimensions or a spontaneously broken gauge symmetry so that such dramatic final states will not occur. Of course if they are seen, we would have to rethink the loopholes to check whether such events could arise from black holes.

However, even if black holes don't provide dramatic global quantum number-violating decays, we expect an observable signal. We focus first on the two jet signal, but we will also show that the two lepton final state can be very helpful in distinguishing among quantum gravity models. One reason we first focus on the jet final state is that we don't know how gauge charge is shed. Since the dominant parton initial state will be quark-quark or gluon-gluon or gluon-quark, we need to know how gauge charge flows. If it is shed in soft quark or gluons from the initial partons, a neutral black hole could be produced in which case the two jet final state would be expected at about ten times the rate for leptons, though the lepton background is smaller so more detailed studies of leptons can be performed even with lower cross section. However, if the initial state carries gauge charge (remember we are dealing with low entropy black holes that decay instantaneously), we would expect a two jet but not a lepton final state.

However, even though the cross section might increase over that of the Standard Model, it might appear that finding black holes or even effects of strong gravity will be difficult if they are only revealed in two body final states since the two jet background would have to be rather precisely predicted. We show that because the jets will have a much more transverse distribution than QCD background, which is dominated by t-channel exchange, the new events would be readily distinguishable. In fact, this difference in angular distribution is a feature of any contact operator due to strong interactions. Because we are not yet safely in the classical gravity regime, we will also consider the possible interpretation of black hole and strong gravity effects in terms of higher-dimensional contact terms generated by strong dynamics. We now exploit this similarity to suggest a new way to search for interesting effects from quantum gravity. This 2 body final state is interesting since there is almost certainly a bigger reach than for multibody final states which are in any case very unlikely to be thermal and because this is truly the quantum gravity regime where classical predictions don't apply. Although we can't predict the results from first principles, the measurements at the LHC can in principle distinguish different models of quantum gravity as we demonstrate below.

With QCD, the $2\rightarrow 2$ scattering cross section at high energies is very forward peaked because of t-channel gluon exchange. When looking for new physics, it is therefore useful to look at both $d\sigma/dM$ and the angular distribution of the decay products. To optimize the search for deviations from the standard model, it is useful to define a quantity R_η [29], which is the ratio of the number of events with pseudorapidity between 0 and 0.5 divided by that for pseudorapidity between 0.5 and 1.0. $R_\eta \equiv N_{events}(0 < |\eta|) < .5)/N_{events}(.5 < |\eta|) < 1)$ Deviations from the asymptotic QCD value of 0.6 would indicate new physics. The quantity R_η is useful because in measuring $d\sigma/dM$ there are a great deal of systematic uncertainties coming from for instance understanding the jet energy, resolution etc, which means that in searching for new physics such as compositeness in dijets $d\sigma/dM$ is not necessarily a reliable quantity. However in the ratio R_η most systematic effects cancel and thus the error is reduced to being essentially statistical only. The variable R_η which originally was used at

D0 [29] has thus been carried over for LHC studies at CMS [30].

We will use this description to interpolate between a notion of some new strongly coupled physics prior to true thermal black hole formation compared to just a sharp turn on of classical black hole production. Clearly the two body final state cross section is enhanced by strong gravitational effects, even before we reach the true black hole threshold.

In fact, virtual black holes are only one type of quantum gravity effect that might lead to changes in the 2→2 scattering cross section. We now list some possibilities, consider constraints in the following section, and how experiment might distinguish among the possibilities in the sections that follow.

We will also consider the role that lepton final states can play in distinguishing among possibilities.

4.1 Quantum Gravity and 2→2 Scattering

No matter what the theory of quantum gravity, the 2→2 scattering cross section might well be the first clue of low-scale quantum gravity and can furthermore yield insight into quantum gravity behavior. Our point is not that any one of the behaviors we consider necessarily applies but that we should be able to experimentally distinguish among them according to the differential cross section and angular distribution of both jet and leptonic final states. There is a great deal of physics that can be done with dijet final states that has been largely neglected up to now. We now consider several possibilities.

Even knowing nothing a priori about quantum gravity it is difficult to imagine no enhancement of the two body final state cross section at scales close to those at which the black hole cross section turns on. If a string theory description does not apply, one might expect a particle description does. The only way to avoid two body final states would be an instantaneous decay into some minimum number of particles. But if we describe the decay through a higher dimension operator as might be appropriate in a particle description, it is clear that the operator coefficient would be so enhanced that even closing off the final states through loops to make a two particle final state, there would still be a sizable decay into two body final states. If a weak string description applies, we expect effects of the sort we soon consider. If, however, string theory is strongly coupled, we cannot predict the behavior but can again see what experiment might tell us. In this case it is reasonable to expect that 2→2 processes are enhanced as we approach the black hole scale, where we mean the scale at which strongly interacting gravity gives rise to truly thermal black holes. At smaller energies it is reasonable to expect hard scatterings due to multigraviton exchange.

Our discussion of two body final states as an indication of black hole production contrasts with Ref. [5], which argues that the 2-body final state is diminished when high multiplicity final states dominate black hole decay. We do not dispute this conclusion applies at high energy, but point out we expect a range of energy at or about the Planck scale for which the two body final state dominates and increases the 2→2 cross section over that of the Standard Model.

4.1.1 Dijet "Black Holes"

According to black hole formulae, we expect an increase in the 2→2 cross section near the black hole threshold. Of course, eventually multiparticle states would dominate as black holes are produced at sufficiently high energy, cutting off the 2 body final state [5]. But sufficiently close to threshold we don't expect this to happen. Even though the classical formula does not apply and we don't truly expect a black hole, we expect enhancement of 2→2 that we model according to the black hole cross section near threshold. This gives

$$\sigma(\sqrt{\hat{s}} > x_{min}M) \approx \pi r_S^2 P_2 \tag{4.1}$$

$$P_2 = e^{-\langle N\rangle} \sum_{i=0}^{2} \frac{\langle N\rangle^i}{i!} \tag{4.2}$$

Note that other authors [3] treat the final decay as a 4 stage process, with balding, spindown, Hawking radiation, and the final explosion. In practice however the existing black hole generators [31, 32, 33] only incorporate hawking radiation and the final evaporation. Our point of view is that "black holes" produced near threshold decay instantaneously, where the average number of particles can be approximated by a Poisson distribution [27, 18]. Note that the most recent black hole generators [31, 32] always have at least two particles in the final state of the decay (unless a remnant is postulated as an option as in [31] a possibility we think unlikely given the results of [34]), so they will never have the two body final states we are looking at unless Hawking evaporation is entirely absent ([33] leaves this as a parameter and can potentially examine 2 body final states). The probability for $\langle N\rangle$ we assign, which is computed assuming Hawking radiation and a Poisson distribution, is probably not accurate. Nevertheless it is a rough approximation to the real probability of a $2 \to 2$ process that we expect to occur and in some sense a conservative estimate since we do not demand that the probability is 1 for low energies.

We note that we don't know how to treat interference since we are in a nonperturbative regime. In our results below, we simply add the Standard Model and black hole cross sections.

Note the distinctive features of this model visible in Figure 7. First of all, we see that the cross section turns on suddenly. Of course this is a consequence of our approximation of sudden turn on at threshold but even allowing for some smoothing we would expect a more dramatic rise in cross section than with higher dimension operators for example as we will show below. The rapid rise would be expected if the black hole is a resonance, or a convolution of a continuum of resonances that might occur near the quantum gravity scale.

This rapid rise in cross section is mimicked in the parameter R_η which measures the angular distribution. We would see the QCD value of 0.6 suddenly jump to a larger value, indicative of a much more transverse distribution. As expected, the two jets due to black holes are far more transverse than the QCD background. The more rapid deviation from QCD could help distinguish black-hole type behavior from other strongly interacting physics. Of course, this rapid turn on was based on our assumption that the black hole event rate takes over at $x_{min} = 1$ (here we mean just our 2 body final state and not the true thermal

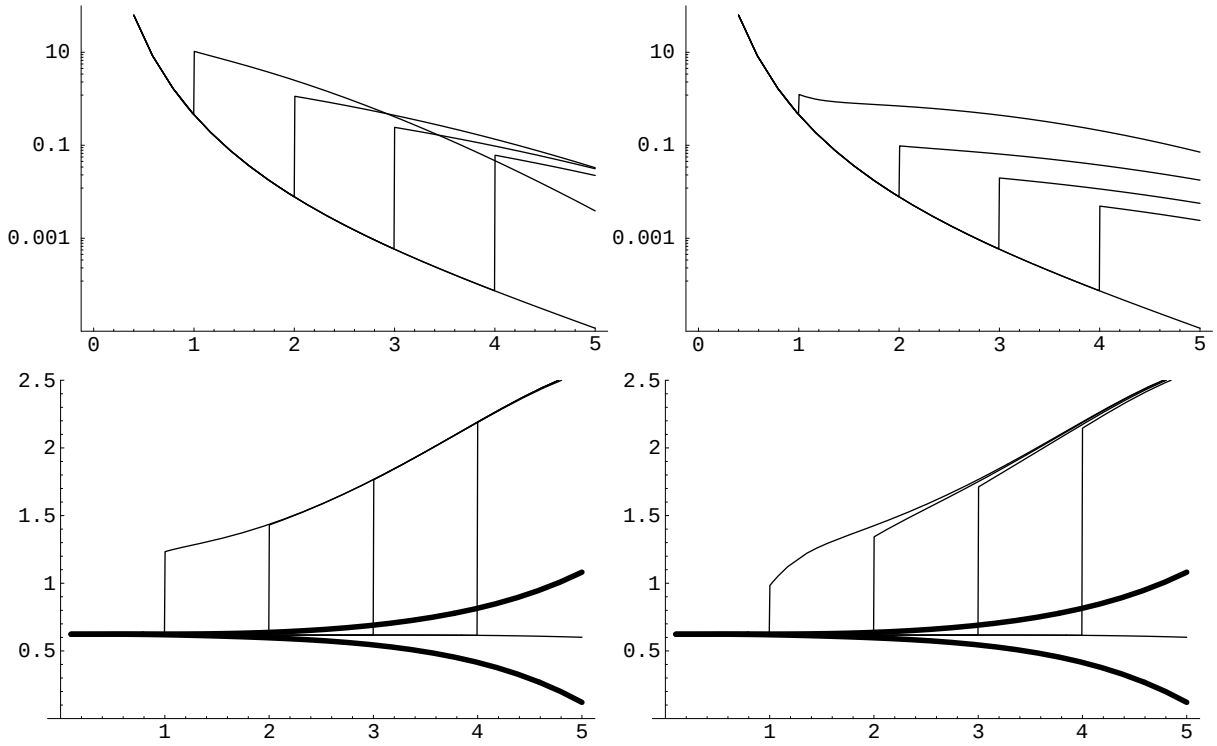

Figure 7: In the upper plots $d\sigma/dM_{jj}$(units of pb/GeV) vs $M_{jj}(TeV)$ is plotted for the case of SM QCD background, and a n=6 ADD model "black hole" behavior with M_D=1,2,3,4 TeV and $x_{min} = 1$ in the lefthand plot and a RS1 black hole behavior with $\tilde{M} = 1, 2, 3, 4$ TeV and $x_{min} = 1$ in the righthand plot. For other values of x_{min} the curves simply start at the corresponding dijet mass. In the lower two plots the R_η is plotted for the same parameters.

black hole). In reality, we expect a smoother interpolating behavior. Nonetheless, it would be very bizarre strong physics other than gravitational that would have a sudden (or even smoothed out) jump at higher energies. One would need a model of strongly interacting physics that turns on in the UV but whose effects disappear in the IR.

The apparently discontinuous jump in R_η reflects the fact that when the "black hole" cross section turns on it dominates QCD and there is no interference. If one were to extrapolate below $x_{min} = 1$ to the regime where interference effects could potentially be visible one finds a different behavior as seen in Figure 8. In Figure 8 with no x_{min} value chosen, one sees that at high energies various values of $\tilde{M}[M_D]$ look identical whereas there is a difference at low dijet masses. This is because even including SM processes black holes dominate at high energies and the angular dependence is that of an isotropic distribution governed by the PDFs. At low dijet masses if there were interference with the black hole cross section (4.1) QCD is competitive and one can see the different scaling of $E/\tilde{M}[M_D]$ for different choices of the Planck scale.

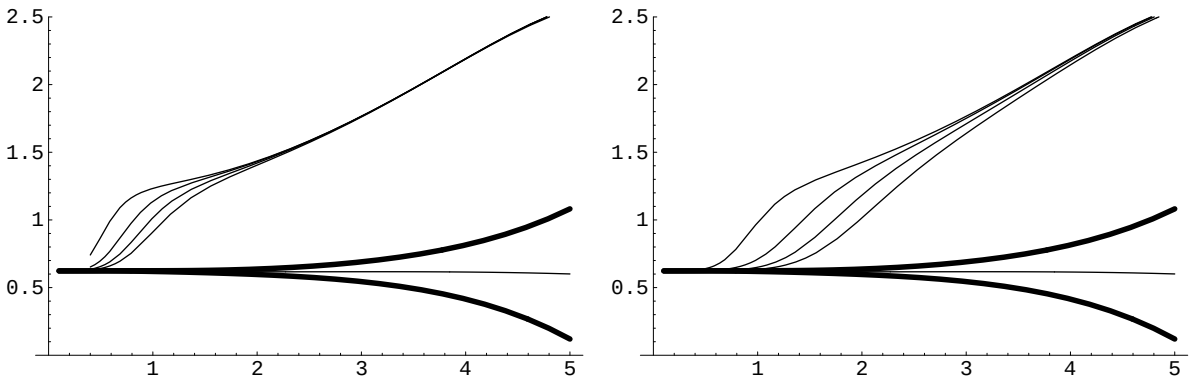

Figure 8: In the upper plots $d\sigma/dM_{jj}$(units of pb/GeV) vs $M_{jj}(TeV)$ is plotted for the case of SM QCD background, and a n=6 ADD model "black hole" behavior with M_D=1,2 TeV and $x_{min} = 1$ in the lefthand plot and a RS1 black hole behavior with $\tilde{M} = 1, 2$ TeV and $x_{min} = 1$ in the righthand plot. For other values of x_{min} the curves simply start at the corresponding dijet mass. In the lower two plots the R_η is plotted for the same parameters.

4.1.2 Stringy Behavior

We have so far assumed the string coupling is of order unity and that black hole like behavior will appear without any obvious signs of a string theory regime. However, if the string scale is low and the coupling is weak, string theory could give rise to resonances that would change the differential cross section and R_η.

In the case of weakly coupled string theory it is well known that above the string scale, the two body final state is reduced exponentially at any large transverse angle. In practice, we expect power law suppression for values of g that are not too small since for sufficiently high genus the loop string contribution will no longer be exponentially suppressed [35] (the behavior is of the form $g^{2G}s^{G+1}e^{-s/(G+1)f(c)}$, where $f(c)$ gives the dependence on angle). Nonetheless, we do expect a dip at high energies that we will explore.

Given a string realization of higher dimensional gravity, be it ADD or RS, there could be additionally a regime of string ball production [36] between the scales M_s/g_s and M_s/g_s^2 at which point black holes start to be produced in light of the BH string correspondence [28]. The cross section for string ball production are interesting in and of itself [36], but one only gets a parametric separation of the black hole and string ball scales when looking at a weakly coupled string theory, which is probably not the case for RS in the IR. With an $\mathcal{O}(1)$ string coupling, all the scales would be about the same and one goes directly in BH production above the scale M. In any case, string balls are relevant only in the weakly coupled regime where black holes would be out of reach.

We now consider string resonances. These resonances, even if too wide to be seen explicitly in the cross section, will also affect the angular distribution and lead to a rise at energies of order the string scale. So probing the ratio R_η can give a detailed exploration of a weakly coupled string theory.

We now assume a model in which the Standard Model 2→2 cross section is modified by a Veneziano-amplitude-motivated form factor:

$$A_{pp\to jj} \equiv A_{SM} A_{ST} \tag{4.3}$$

$$A_{ST} \equiv \frac{\Gamma\left(1 - \frac{s}{M_S^2}(1+i\gamma)\right)\Gamma\left(1 - \frac{t}{M_S^2}(1+i\gamma)\right)}{\Gamma\left(1 - \frac{s}{M_S^2}(1+i\gamma) - \frac{t}{M_S^2}(1+i\gamma)\right)} \tag{4.4}$$

yielding the results for the differential cross section and R_η shown in Figure 9.

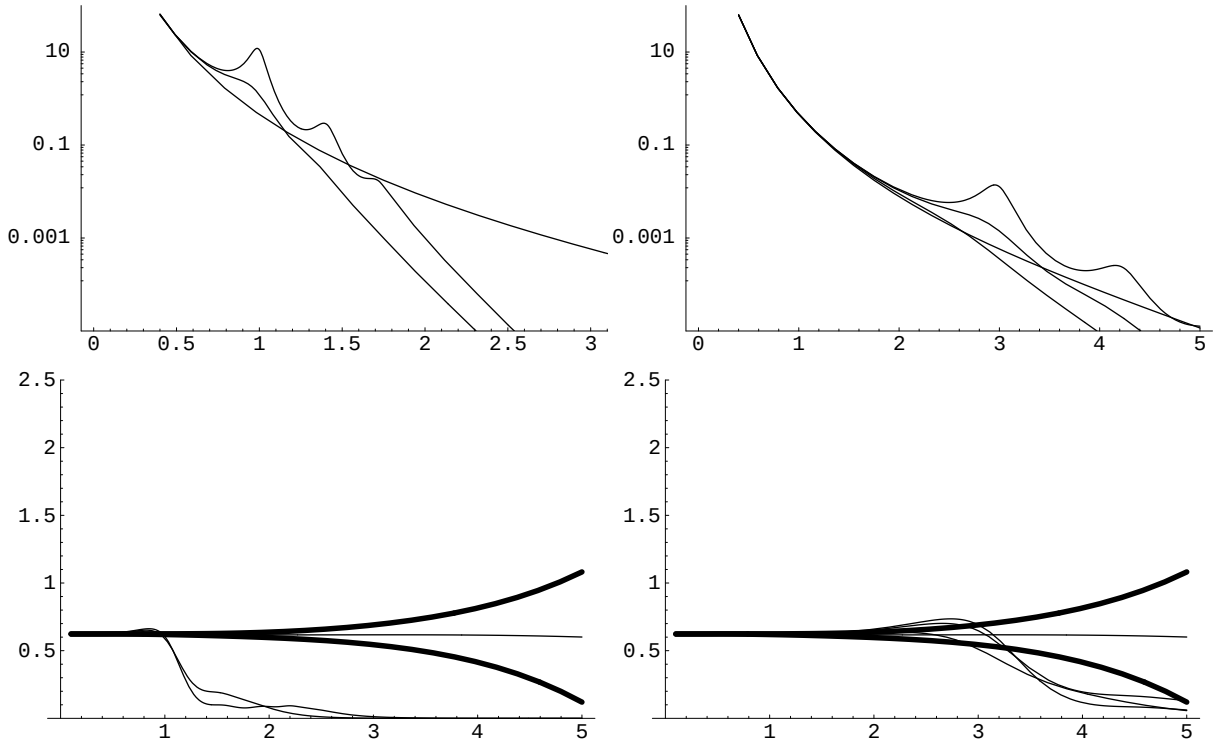

Figure 9: In the upper plots $d\sigma/dM_{jj}$(units of pb/GeV) vs $M_{jj}(TeV)$ is plotted for the case of SM QCD background(thicker curve), and a toy stringy behavior with M_s=1 TeV in the lefthand plot with $\gamma = .1, .3$ and M_s=3 TeV in the righthand plot with $\gamma = .1, .3, .6$. In the lower two plots the R_η is plotted for the same parameters.

We see the characteristic string behavior. First of all we see several resonances appear at about the string scale. Furthermore, we see the 2→2 cross section decrease in the region of η we have considered. But the most notable and characteristic feature of string behavior would be the much less transverse behavior of the 2→2 cross section (exactly the opposite of what we considered with black holes in the previous subsection). We see this dramatically illustrated in the lower plots, where R goes from the QCD value of 0.6 (or higher when there are resonances) down to essentially 0. In Figure 10 we have included statistical errors on

R_η and we see that although R is close to zero, there are enough events to trust this value. That is, we can see the string theory dip in the regime where there are sufficiently many events to trust the result.

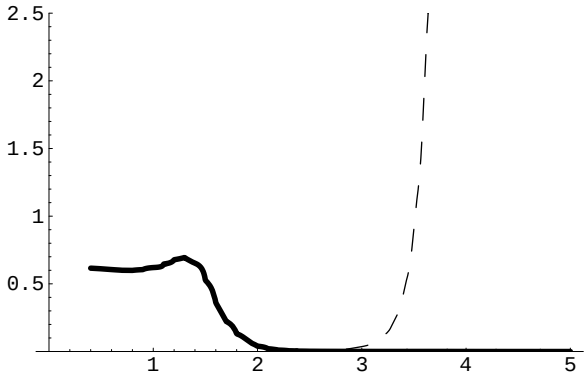

Figure 10: R_η is plotted for $M_s = 1$ TeV and $\gamma = .1$ for the amplitude defined with (4.5) with one sigma gaussian error bars corresponding to 1 inverse femtobarn of luminosity.

It is also interesting to note that this dip allows us to readily distinguish string theory from other models with resonances, such as a colored octet resonance, as illustrated in Figure 11. Even when $d\sigma/dM$ is rather similar, R reverts to the QCD value away from the resonance for the octet but drops off for string behavior. In fact, the resonances might not appear explicitly if they are too wide but we would still be able to ascertain the presence of stringy physics.

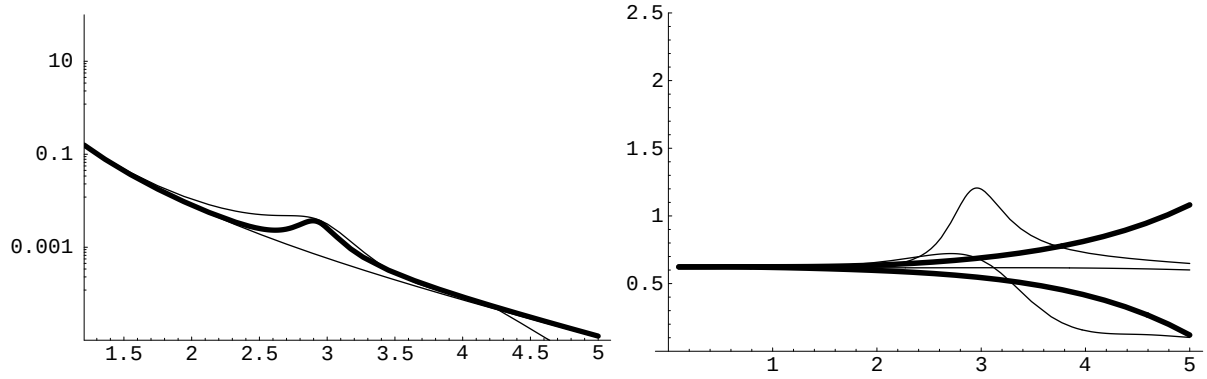

Figure 11: In the left plot $d\sigma/dM_{jj}$(units of pb/GeV) vs $M_{jj}(TeV)$ is plotted for the case of SM QCD background, a toy stringy behavior with M_s=3 TeV and $\gamma = .2$ and a massive colored octet resonance(thicker curve) with mass and width chosen to mimic the differential cross section behavior near the resonance. In the right hand plot the same curves are plotted for R_η, note the easily discernible difference between field theory resonance and "string" theory resonance.

Finally, we show the somewhat notable result that with both the differential cross section and the angular distribution we can distinguish different stringy form factors.

$$A^0_{ST} \equiv \frac{\Gamma\left(1-\frac{s}{M_S^2}(1+i\gamma)\right)\Gamma\left(1-\frac{t}{M_S^2}(1+i\gamma)\right)}{\Gamma\left(2-\frac{s}{M_S^2}(1+i\gamma)-\frac{t}{M_S^2}(1+i\gamma)\right)} \tag{4.5}$$

For example, with the original Veneziano amplitude (4.5), there is no angular dependence in the first resonance. Even though there is a resonance appearing in the differential cross section, it doesn't show up in R_η, as demonstrated in Figure 12. This would be a clean way to distinguish the two different forms of the Veneziano amplitude, one which appears in supersymmetric theories (4.4) and the original amplitude (4.5).

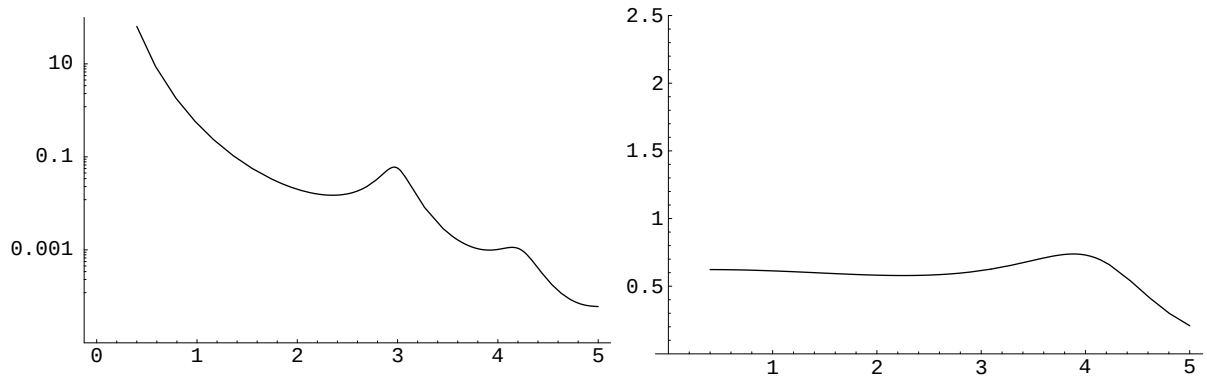

Figure 12: In the left plot $d\sigma/dM_{jj}$(units of pb/GeV) vs $M_{jj}(TeV)$ is plotted for the case of SM QCD background(thicker curve), and a toy stringy behavior (4.5) with M_s=3 TeV and $\gamma = .1$. In the right hand plot R_η is shown for the same parameters.

4.1.3 Higher-Dimension Operators

Finally, strong gravity effects can give rise to higher dimension operators that exist well below the gravity scale. The lowest dimension operator would of course have dimension 6 but higher dimension operators should also exist and be competitive when near the gravity scale. The effects of these operators can in some ways resemble that of black holes-that is lead to a rise in cross section above that of QCD and also give rise to much more transverse events. However, there can be interesting features that would distinguish these different contributions.

First is that the energy dependence of any particular higher-dimension operator is distinctive, and can in principle differentiate these operators from the "black hole" contribution we described and from each other. As we will see when comparing he higher dimensional results to the figures in Section 4.1.1, this distinction will be most manifest in the low energy region where the interference terms bring out the energy dependence that is otherwise lost in the PDFs.

The second difference is that we assumed true black hole type effects would have a threshold at about the quantum gravity scale but have form factors that kill them at low energy. Higher-dimension operators will by our assumption be those that survive to low energy. Of course, it is possible that "black holes" are responsible for higher-dimension operators that cut off at low energy (or similarly grow rapidly above a certain scale as in [37]). In this case, they would be very much like black hole type effects already considered and would similarly cut off at low energies.

Although all higher-dimension operators might be relevant at the LHC if the quantum gravity scale is low, we will focus on four-fermion operators which are adequate to illustrate our point. If the quantum gravity scale is high, it is appropriate to keep the lowest dimension operator. If it is low, it would give a qualitative sense of the behavior of the 2→2 cross section. The precise energy dependence can be quite different, but this would nonetheless look similar at higher invariant mass where the operators would dominate over QCD so interference terms would be insignificant. The current bound on the scale suppressing a four fermion quark operator $(q_L\gamma^\mu\bar{q}_L)^2$ where $q = u, d$ is $\Lambda = 2.7$ TeV [16] assuming a coefficient of 2π for the operator. CMS studies show that the mass scale that can be probed at the 95 % C.L is $\Lambda \sim$ 15 TeV while at the 5 σ discovery level it can discover effects from $\Lambda \sim 12$ TeV with 10 inverse femtobarns of data.

In this regime one might also question the legitimacy of a higher dimension operator parametrization. Over some of the energy regime we are below the scale in the denominator. Of course the answer depends on whether there are any small coupling factors etc. We view this as a model. If the scales are comparable higher order operators become relevant and eventually the expansion breaks down altogether. But as the energy scale is not too far from the denominator scale being probed, this shouldn't be too bad a model.

To find the form of the assumed four-fermion operators, we assume that black holes respect gauge symmetries, but not necessarily global symmetries. However, if we were to write down arbitrary operators at the TeV scale generated by black holes then we would immediately be ruled out by for instance proton decay and flavor bounds. Thus we restrict the set of operators that we are interested in to the lowest dimensional operators that preserve the good symmetries of the SM. This is of course a reasonable assumption as we are inherently in the quantum gravity regime and whatever theory this amounts to necessarily incorporates the symmetries of the SM if the scale of quantum gravity is possibly near the TeV scale. This leaves us with dimension 6 operators of the form

$$\sim \frac{c}{\Lambda^2}\Sigma(\bar{f}\gamma^\mu f)^2. \tag{4.6}$$

Furthermore, the four fermion operator automatically accounts for overall "black hole" spin through its Lorentz structure whereas in the black hole case one has different types of black holes with different spins. One advantage of the four-fermion approach is that it automatically takes into account the constraints of spacetime symmetries. The four fermion operator automatically produces the final states allowed by Lorentz symmetries (symmetries which are violated by the classical black hole).

In addition to black holes with different angular momentum, black holes could in principle

carry different gauge charges. Again, the four fermion operator and black hole would account for these in different ways. In the four fermion case, it is a question of how gauge indices are contracted. In general, for the black hole, we assume it is charge neutral but this is not necessarily the case since charged partons might collide to form the black hole.

As suggested above, the four-fermion operators might arise from black holes or virtual black holes or some other nonperturbative gravity effect. Higher-dimension operators might also arise from perturbative loop calculations as demonstrated in Ref. [8] for example.

Four-fermion operators might also arise as virtual effects from string theory at energies below the string scale. In fact, the Veneziano amplitude (4.5) includes an operator that would be accounted for by a four-fermion operator in its expansion (that is an operator, with amplitude scaling as s/M_S^2. However, the alternate form for the Veneziano amplitude that arises in supersymmetric theories (4.4) does not have this term and the first higher dimension operator enters at dimension 8. So as we will see, exploring the energy dependence of the differential cross section and R could distinguish these possibilities. A particular example of modern string models with dimension 6 operators can be found in [11] which can be compared with the dimension 8 operators found in [9, 10].

Finally, string theory can give rise to harder scattering if in warped space [39]. Whereas perturbative string theory in flat space would cut off the 2→2 scattering amplitude, perturbative string theory in warped space is dual to a strongly interacting conformal field theory that would give rise to hard scattering amplitudes. Ref. [39] discusses how in curved space, hard QCD-like behavior is reproduced in string theory, even though the naive flat space expectation is that it does not. Moreover Bars and Hinchliffe [41], in their analysis of toy string models for the SSC, have noted that if a string theory acted like a QCD string then it would not demonstrate the dip in 2 body final states characteristic of weakly coupled string theory in flat space. Additionally taking into non-perturbative string states as in [40] could also produce harder scattering than the naive flat space suppression of the string scattering cross section, though for perturbative string theory this is a small effect.

Of course the precise connection between the scale in the denominator of the four-fermion operator and M_D is model dependent and in general unknown, as we will make even clearer in the following subsection. Nonetheless, it is worthwhile looking for such effects and distinguishing them from the other types of quantum gravity behavior we have described.

So we consider a four-fermion operator of the form [42, 43]

$$\frac{1}{2\Lambda_{QG}^2}(\bar{\psi}_L\gamma^\mu\psi_L)^2 \tag{4.7}$$

Here we see the differential cross section and R_η scale as in Figure 13. Furthermore we can also potentially see signals in the lepton channel as will be discussed in Section 4.2.

4.2 Leptonic Final States

We have so far concentrated on jet final states which have the biggest cross section. However, leptonic final states can be very important as well and can be critical to distinguishing among

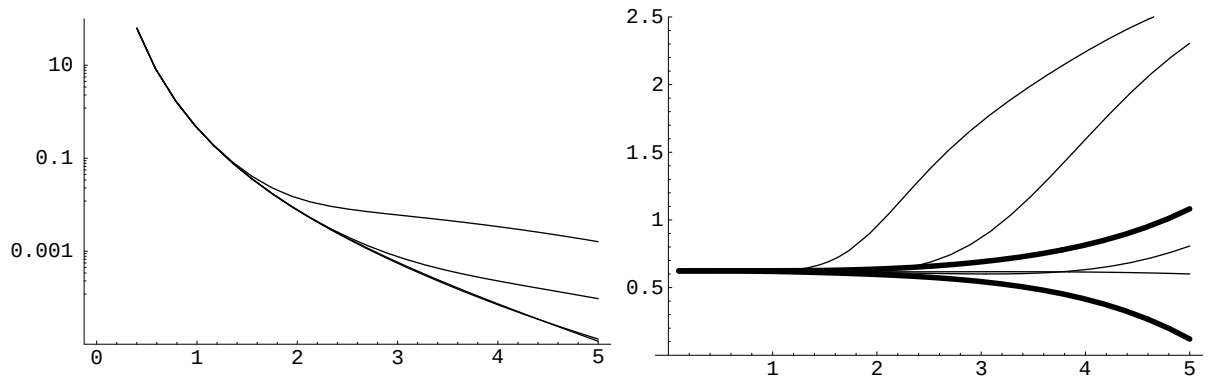

Figure 13: In the left panel $d\sigma/dM$(units of pb/GeV) vs M_{jj}(TeV) is plotted for QCD(the lowest curve) and a set of four fermion operators with $\Lambda = 1, 2, 4$ TeV. In the right panel R_η is plotted for the same operators as well as QCD with the statistical error bars for QCD are overlaid for 1 fb^{-1} of data.

quantum gravity models. Leptons are generally clean enough at these high energies that identifying new physics doesn't necessary require studying the angular dependence. But for a black hole or quantum gravity-related signature, we expect the same energy dependence for the leptonic and hadronic final states.

The most interesting feature of the leptonic final state will be the relative cross sections for leptons and quarks. The relative ratio would be different for a classical thermal decay (for which it is about 10 %) relative to the decay due to a four fermion operator, for example, for which the relative rate is about 20 %. In the first case, the relative rates depend only on the number of species and the multiplicity due to spin counting whereas in the second case the numbers depend on number of species but also on the dimension of the associated field. For example, gauge bosons associated with a field strength would be suppressed relative to fermions. Although the first operators including a field strength arise at dimension five $\bar{\psi}\psi\sigma_{\mu\nu}F^{\mu\nu}$ they are chirally suppressed (proportional to the light fermion mass). Relative numbers of leptons vs quarks could also in principle depend on whether the quarks and leptons are slightly split from each other in a higher dimension, so a deviation from naive predictions might indicate something about the structure of the underlying theory.

But even more important than this counting is the way charge flows. A black hole can in principle be formed from a color charged initial state, namely two gluons or two quarks. The leptonic fraction will then be 10 % of the total black hole two body decay rate.

The four fermion operators on the other hand would have to be $q\bar{q}\ l\bar{l}$ type operators which means that only the q and $\bar{q}$ initial states will contribute. Because the PDFs for $\bar{q}$ are so much smaller, the relative fraction of leptonic final states will be much smaller. In addition, the four fermion operator has an additional $\hat{u}/\hat{s}$ type suppression which is relevant because we are focusing on the central region. Finally a true four fermion operator will appear with an additional alpha because the interference dominates. The upshot is that the leptonic contribution from four-fermion operators is down by about a factor of a thousand.

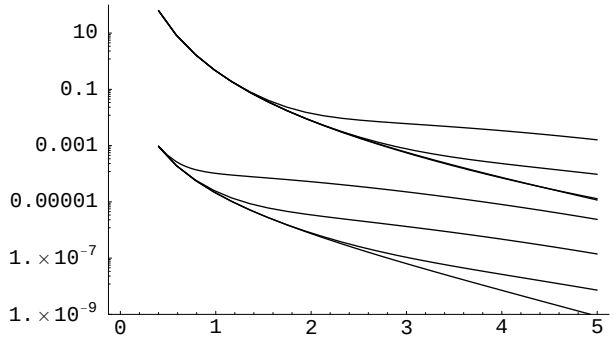

Figure 14: $d\sigma/dM$(units of pb/GeV) vs two body invariant mass(TeV) is plotted for QCD(the lowest curve) and a set of four fermion operators with $\Lambda = 1, 2, 4$ TeV for di-jets in the upper curves. In the lower curves SM Drell-Yan production of leptons is plotted in combination with a four fermion operator that generates a l^+l^- final state with various $\Lambda = 1, 2, 4$ TeV.

Nonetheless CMS studies show that the mass scale that can be probed at the 5 σ level can be as large as 23 TeV for dimuons [38] and 12 TeV in dijets [30] for 10 inverse femtobarns (where the coefficient of the operator is 2π). The current strongest bounds from low energy experiments are 4.2 TeV for dimuons and 2.7 TeV for dijets [16]. This means that we might hope to distinguish various possibilities through a joint measurement of lepton and jet final states. In Figure 14 we plot the Drell-Yan background and the effects of a $q\bar{q}\ l\bar{l}$ operator as well as the dijet operators from Section 4.1.3 to show a comparison of rates for several values of Λ.

Another possibility is that a black hole that will give rise to the states had to be formed from a neutral state but didn't have either the α or $\hat{u}/\hat{s}$ suppression factors. It is also possible that a charged final state is also of interest. A u and $\bar{d}$ initial state or the charge conjugate could give rise to a charged state that can decay into lepton and neutrino. We expect this final state to dominate above background as the neutral state does. In Figure 15, we plot these possibilities and see the significant difference in overall rate that can be used to distinguish among possibilities.

5 Conclusions

In this paper we have argued that if the higher-dimensional gravity scale is indeed low, we are likely to learn more and sooner about quantum gravity from studying two particle final states than by studying multiparticle decays from higher-dimensional black holes. Although we haven't precisely determined the reach, we expect in all cases to be able to probe to scales of order 5 TeV by looking at the two particle final state channels.

We find it very unlikely that the LHC will produce conventional black holes. In almost

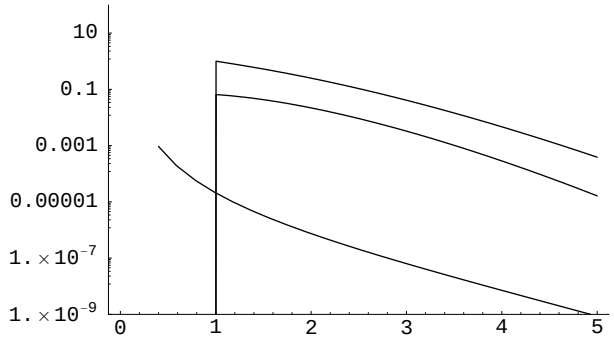

Figure 15: $d\sigma/dM$(units of pb/GeV) vs two body invariant mass(TeV). The curves from top to bottom represent black hole cross section for $M_D = 1$ TeV , $n = 6$, and $x_{min} = 1$ for a black hole decaying into l^+l^- (assuming any initial gauge charge is radiated softly), black hole cross section for $M_D = 1$ TeV and $x_{min} = 1$ for a "charged" black hole decaying into $l\nu$, and the lowest curve is the Drell Yan background.

all cases the entropy is too low to trust there is actually a black hole final state. In particular we found even if we assume we are in the black hole regime that low multiplicity final states dominate, and the two body final state should be particularly interesting.

We have found a number of interesting features that can be used to distinguish among the possibilities for quantum gravity effects. We have shown that by studying both the differential cross section and the transversality parameter R_η as a function of energy we can identify new effects and distinguish among black hole type cross sections, perturbative string theory, and higher dimension operators.

We have furthermore noted a number of specific points. The relative lepton fraction can provide very valuable information. It is likely to be large only in the case that black hole resonances that shed gauge charge form. Otherwise the parton distribution functions suppress the rate.

Furthermore we have found that we can distinguish string resonances from other resonances and furthermore distinguish among different string models.

We have found that black holes and four fermion operators differ in their threshold behavior and that furthermore by studying the threshold regime where interference is relevant one might be able to distinguish different energy dependencies of various operators.

There are a number interesting follow up studies to consider. On the theory side, it would be nice to consider various string models and their predictions. Although initial work on string theory [9, 49, 11, 10] studied 2→2 scattering, it would be interesting to see the predictions of string models which have been developed in the interim. It would also be interesting to study threshold black hole behavior if at all possible.

Other more phenomenological studies include seeing how much information can be gleaned from the transversality or sphericity of multibody final states. In particular, even if there is missing energy or other jets, it might still be of interest to study the two leading jets.

Finally a more detailed experimental analysis of how well one can distinguish among different models would be very useful.

Acknowledgments

We would like to thank Nima Arkani-Hamed, Tom Banks, Csaba Csáki, Greg Landsberg, Lubos Motl, Alberto Nicolis, and Lenny Susskind for useful discussions and Greg Landsberg for sharing his results and a careful reading of our manuscript. The work of PM and LR is supported in part by NSF grants PHY-0201124 and PHY-0556111.

A RS Black Holes

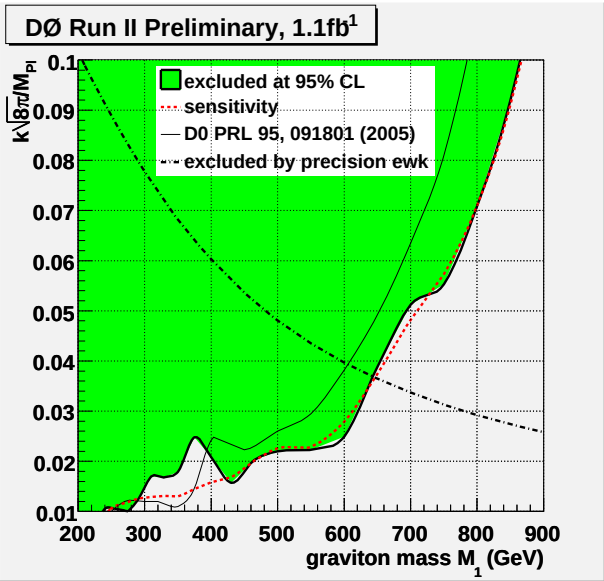

Figure 16: Recent D0 search results from 1 inverse femtobarn of luminosity updating the results of [44].

We start with the convention for the RS1 normalization

$$\frac{M^3}{2}\int d^5x\sqrt{g}R \tag{A.8}$$

which leads to the familiar relation

$$M_{Pl}^2 = M^3/k(1-e^{-2kr_c}) \tag{A.9}$$

where M_{Pl} represents the reduced Planck mass, and r_c is the size of the extra dimension. To determine the relevant parameters for black hole production in RS1 we need to reinterpret

the commonly used parameters k/M_{Pl} and m_1 (the first kk graviton mass) in terms of the fundamental five dimensional Planck scale, M, and the AdS curvature k. The most current available bounds on RS graviton production from the D0 experiment are given in Figure 16. For a given value of $k/M_{Pl} \equiv c$ and m_1

$$\tilde{M} = \frac{m_1}{x_1 c^{2/3}}, \tag{A.10}$$

where $x_1 = 3.83$. Thus if we were to extend $k/M_{Pl} \sim .5$ and take 1000 GeV as the approximate bound for m_1 we get $\tilde{M} \sim 350$ GeV. Choosing $k/M_{Pl} \sim .5$ means that the strong coupling scale is extremely close to k so to be somewhat more conservative we use $\tilde{M} \sim 500$ GeV as the lower bound that we have used throughout this paper when computing the RS black hole cross section.

We now discuss what types of black holes exist in the context of RS and their potential phenomenological implications. Black hole solutions in Randall-Sundrum models have been studied for both RS1 and RS2 variants [50]. In studying RS black holes in experiments the only relevant solutions are those in RS1 where there is an IR brane with the SM localized there. The reason for this is that in models without an IR brane the SM feels the usual Planck scale, while in RS1 there is a warp factor that can allow for an effective Planck scale of $\mathcal{O}$(TeV) One can consider variants of this situation (see [48]for example) with light fermions and gluons in the bulk but this will greatly suppress the black hole production cross section, since they can be produced only at or near the TeV brane.

For RS1 black holes there are essentially two different regimes that are relevant– unlike flat space BHs. In flat space one can analyze black holes with Schwarzschild radius less than the compactification radius and there is only one type of solution. In RS1 since the bulk is warped with a scale set by the AdS curvature k, there are separate regimes when $r_S << 1/(ke^{-kr_c})$ and when $r_S \geq 1/(ke^{-kr_c})$ where curvature is relevant. In the first case where $r_S << 1/(ke^{-kr_c})$ the black hole can be thought of as a five dimensional flat space black hole, which means the approximate expression for the Schwarzschild radius can be obtained by matching the RS action to the Myers-Perry solution[15] for a d-dimensional Schwarzschild BH. Carrying out this matching one obtains

$$r_S = \left(\frac{M_{BH}}{3\pi^2 \tilde{M}^3}\right)^{1/2}, \tag{A.11}$$

where $\tilde{M}$ is the five dimensional Planck scale. Actually it is subtle to derive this formula since the best way of deriving it is coordinate dependent.

The simplest way to see that we expect five-dimensional RS almost flat space black holes is to work in terms of the parameter $\tilde{M}$ in the first place. Since we are interested only in the region near the TeV brane, the warp factor doesn't even enter (until we get to large distances) so we expect the behavior to be that of five-dimensional gravity with a low Planck scale.

One can also directly match to the Myers-Perry solution using conformally flat coordi-

nates as in [13]. In this case starting with the metric

$$ds^2 = \frac{1}{(kz)^2}\left(dz^2 + dx_\mu^2\right) \tag{A.12}$$

and performing a conformal transformation one is left with the relevant part of the effective gravitational action at the TeV brane

$$M^3\left(\frac{1}{kz_0}\right)^3 \int d^4x dz \sqrt{g} R = \tilde{M}^3 \int d^4x dz \sqrt{g} R, \tag{A.13}$$

where z_0 is the location of the TeV brane in the coordinates (A.12), and $1/z_0 k$ is the warp factor. From the form of this solution it can be easily matched to (2.3) the Myers-Perry solution where the assumption is that the metric is asymptotically flat.

In the commonly used RS coordinates

$$ds^2 = \exp -2ky dx_\mu^2 + dy^2 \tag{A.14}$$

the derivation isn't quite as obvious given that the effective action at the TeV brane is

$$M^3 e^{-2kr_c} \int d^4x dy \sqrt{g} R. \tag{A.15}$$

Thus there would seemingly not be enough powers of the warp factor if we were matching to the Myers-Perry solution to end up with a relevant black hole mass scale of $\tilde{M}$. This should not come as a surprise though as because in looking at fluctuations about a given position in (A.14) the metric is not manifestly 5D flat space. However one can convince oneself that the relevant mass scale for black hole production is $\tilde{M}$ by computing the effective gravitational potential at the TeV brane,

$$V(r) \sim \frac{1}{M_{Pl}^2}\frac{m_a m_b}{r} + \frac{1}{M_{Pl}^2 k \exp -3kr_c}\frac{m_a m_b e^{-m_1 r}}{r^2}. \tag{A.16}$$

Neglecting the first term which comes from the zero mode of the graviton and is negligible at short distances, we see that the second term approximates a five dimensional flat gravitational potential for $r < 1/m_1$. From this one can derive the approximate horizon radius via Laplace by setting the kinetic energy equal to the potential energy (as also done for ADD black holes in [4]) and thus we arrive at

$$r_S \sim \left(\frac{M_{BH}}{\tilde{M}^3}\right)^{1/2}, \tag{A.17}$$

where we have expanded the exponential in (A.16) to the lowest order. Additionally we see that from looking at higher order terms in the expansion we should find deviations from this approximate form at order $r_S \sim 1/k \exp -kr_c$ when we expect curvature corrections to be taken into account. Eventually when the black holes are large enough in size the solution should change to an AdS-Schwarzschild black hole. From these various derivations there are

TeV sized approximate flat space black holes in RS1 and we assume the flat space behavior for the relevant regimes we are interested in throughout this paper.

As in flat space the production cross section for these black holes is given roughly by r_S^2 and would seem to grow unbounded with energy/the mass of the BH. However in the context of RS models we know this behavior has to be modified in some way as the black hole size approaches the AdS curvature length. Additionally one knows that the cross section cannot grow as a power law forever from AdS/CFT reasoning [45][]. In [45] it was conjectured that once you made black holes with size $1/k$ the cross section was bounded and never got larger than this value. However a more refined understanding of what happens at this scale was put forth by Giddings [46], who conjectured from the gauge theory dual side at the scale $1/k$ the Froissart bound is saturated and then the cross section doesn't cease growing but grows as $\ln^2 E$. Interestingly enough Giddings was also able to show that this behavior can be seen directly by looking for BH solutions in linearized gravity and he found that when taking into account curvature effects $r_S \sim \ln E$ strengthening the argument for the Froissart bound $\ln^2 E$ behavior.

Given the additional effects of curvature in RS1 the basic regimes for cross sections can be summarized in the following way

$$\begin{aligned} E > \tilde{M} \qquad & \sigma \sim E/\tilde{M}^3 \\ E \gtrsim \left(\frac{M}{k}\right)^2 \tilde{M} \qquad & \sigma \sim \ln^2 E, \end{aligned} \tag{A.18}$$

thus demonstrating that one gets rather different results than simply a five dimensional flat space black hole depending on the ratio M/k. In practice however this effect is small when M/k is large, as with QCD where you never really see the effects of the softening of the cross section). We also see that we would want M/k to be large to approach the large entropy regime, but this is the regime where experimental constraints are stronger.

This discussion of course ignores the possible effects of any additional scales beyond k and M, for instance an additional scale set by M_s and g_s. It is in principle possible to form string resonances or string balls in this case as well as the truly flat case. Nevertheless as we see from (A.18) the only really relevant parameter for RS1 "black holes" is $\tilde{M}$ given that black holes will dominantly be produced at threshold due to the falling PDFs.

B Existing Constraints on the Quantum Gravity Scale

In the text we have discussed several possible models for quantum gravity effects, including black holes down to low energies, perturbative string theory, and higher-dimensional operators. In all cases it will be difficult to constrain the Planck scale based on nonobservation of these effects, in the first case because of lack of knowledge of x_{min}, in the second case because we don't know the string coupling, and in the latter case, because we don't know how to predict a precise relationship between the Planck scale and the scale occurring in a higher-dimensional operator.

Nevertheless, we do need to consider other searches for the types of operators and effects we have suggested, since in principle they can rule them out over the measurable range. In particular, Giudice, and Strumia as well as Contino et al [8, 47] considered four-fermion operators, while [11, 9, 49, 10] considered constraints on the string scale. In both cases, the constraints appear rather stringent and if true, would significantly impinge on the parameter regime we have considered.

We first consider Ref. [8], who demonstrate that loop effects with KK gravitons exchanged can generate four-fermion operators. They argued that the strong bounds on dimension-6 operators, in particular those involving quarks and leptons, significantly constrain the allowed coefficients of the operator they found. The operator is clearly suppressed by the higher-dimensional Planck scale, M^2, and they chose to interpret the experimental constraint as a constraint on the UV cutoff on the effective theory for which a loop calculation would apply. That is, string resonances or other states might enter at an energy lower then the strong scale determined by nave dimensional analysis, and they put a constraint on the scale Λ for various values of M_D.

This analysis could have an impact on our study for several reasons. First, if the cutoff necessarily occurs below the quantum gravity scale, we would expect $2\rightarrow 2$ scattering to be lower than the simple estimates we presented. Second, independently of their cutoff procedure, if the scale of four-fermion operators is constrained to be the current bound from LEP II on quark lepton operators, the four fermion operators we consider would already be ruled out.

We consider the second concern first. The current strongest bound on the scale of four-fermion operator for $qqee$ with coefficient $4\pi/\Lambda^2$ is $\Lambda = 26.4$ TeV [16]. However, there are several reasons this quark lepton bound might not apply to quantum gravity. The first is that the four quark operator and the quark lepton operator will not necessarily occur at the same scale if quarks and leptons are separated in the bulk, as they might be to address baryon number violation concerns. A second reason this operator might be suppressed is that if the operator is generated by strong gravity, such as effects from black holes, the operator might turn on only at high energy. Of course, this would not be a true four fermion operator that applies to low energies but one with significant form factor suppression at low energy. For the true four fermion operator, if it is generated by strong gravity, it could be that the lepton contribution is suppressed relative to the quark contribution simply because there are fewer leptons coupling to the graviton (and even fewer charged leptons). This would not however prevent the loop contribution which is already nominally too big for leptons. However it is possible that the operator is not as stringent as presented in Ref. [8] because the cutoff for fields on the brane is different than than in the bulk. We now reconsider this analysis.

The scale Λ_S is defined in Ref. [8] as the strong scale at which the gravitational coupling, $g^2 = c_n(\Lambda/M_D)^{2+n}$ (where c_n in their convention for the gravitational action is $(2\pi)^n$) is equal to the loop factor, $(4\pi)^{D/2}\Gamma(D/2)$, where $D = 4 + n$ is the number of dimensions, and we will divide this loop factor into the product $l_4 l_n$, where $l_4 = 16\pi^2$. So we have

$$\Lambda_S = \left(\frac{l_4 l_n}{c_n}\right)^{\frac{1}{2+n}} M_D \tag{B.19}$$

If we were to compute the box diagram with two gravitons exchanged, with the graviton propagator, adding up all the KK contributions, taken to be

$$G(k,0) = \frac{S_{n-1}}{2(2\pi)^n} \int_0^{\Lambda_{KK}^2} dm^2 \frac{(m^2)^{n/2-1}}{k^2+m^2}, \tag{B.20}$$

where

$$S_{n-1} = \frac{2\pi^{n/2}}{\Gamma(n/2)}. \tag{B.21}$$

Yielding the box diagram contribution [8]for the coefficient of the four fermion operator

$$C_\gamma = \frac{15}{64} \frac{c_n^2}{l_4 M_D^{4+2n}} \int_0^{\Lambda^2} dk^2 k^4 G^2(k,0) \sim \Lambda_S^{2+2n}, \tag{B.22}$$

where the scaling in the final expression comes from assuming all momenta are cut off at Λ_S.

Notice that this answer would scale as $c_n^{2/(2+n)}/M_D^2$ as it should for a convention independent answer.

If the authors of Ref. [8] had cut off all momenta at the scale Λ_S, they would have concluded that over a reasonable range of M_D, the strong scale determined by NDA is already excluded. They chose instead to interpret this loop contribution as implying the effective theory must be cut off at a scale lower than Λ_S.

We will interpret the four-fermion operator bound differently and assume the strong scale Λ is a function of the convention-dependent parameter M_D so we interpret the bound directly as a bound on the scale M_D. With this interpretation, we would have a strong constraint on the allowed values of M_D given the loop contribution that Giudice and Strumia computed.

However, in the phenomenological low scale gravity theory of interest with respect to black hole production, the Standard Model particles are confined to a brane whereas gravity propagates throughout the bulk (otherwise production is very suppressed but for a scenario where black holes are investigated with matter in the bulk see [48]). The strong scale in Ref, [8] is based on the bulk particles and isn't necessarily the cutoff for particles on the brane.

In fact, with the cutoff taken to be the strong scale one notices a peculiarity. Let us consider a box diagram with two gravitons exchanged. As Giudice and Strumia point out, you get one integral over four momentum suppressed by the phase space factor $l_4 = 16\pi^2$ and you get two factors of n-dimensional momenta suppressed by two factors of the n-dimensional phase space factor l_n. If we assumed nothing cut off strong coupling, one would find a loop diagram can generate a four fermion operator with coefficient proportional to $1/l_4\Lambda_S^{2+2n}$, which is in turn proportional to $l_4^{n/(2+n)}$. That is, the answer *grows* with the four-dimensional phase space factor, which is very strange from the perspective of NDA. Generally NDA results have phase space suppression in the denominator due to loop integrals, some of which are partially compensated by the strong scale, but never so as to grow with the phase factor.

The resolution to this puzzle presumably has to do with the fact that we are considering dimension six four-fermion operators in the first place. They are living only on the three

plus one dimensional surface of the brane. So although the integral is higher dimensional, we expect that at least the additional n-dimensional momentum integral should be cutoff in the transverse directions by the size of the brane. So an alternative NDA estimate is obtained by factoring the phase space into the directions along the brane and the orthogonal directions.

One then finds the result scales as

$$\frac{15}{64}\frac{\pi^n c_n^2}{16\pi^2(2\pi)^n\Gamma(n/2)^2}\frac{\Lambda_S^2\Lambda_{KK}^{2n}}{M_D^{4+2n}} \tag{B.23}$$

The bound on the quantum gravity scale can be considerably relaxed when the cutoff in the orthogonal directions is lower than Λ_S since Λ_{KK} can be smaller than Λ_S. For example, for $n = 6$, $\Lambda_S = 1.8M_D$ whereas if $\Lambda_{KK} = M/c_n^{1/(2+n)}$ (the convention-independent quantity) we have $\Lambda_{KK} = .25M_D$. Since Λ_{KK} is raised to the twelfth power, this gives a considerably smaller result. Similarly, with $n = 1$, we have $\Lambda_S = 4.9M_D$ and $\Lambda_{KK} = 0.54M_D$. This is raised to the fourth power, again considerably suppressing the final result. Of course Λ_{KK} can be bigger, but still satisfy the bound. For a strong gravity theory, even without an explicit cutoff, we don't know whether the gravity theory would actually apply to scales Λ_S which are bigger than M_D in any case.

So we conclude that existing four fermion operator constraints are serious but do not necessarily rule out the allowed parameter space. It is therefore worthwhile to look for compositeness effects of the type we described.

We now briefly turn to possible existing string bounds, which are highly model-dependent. For example, Antoniadis [11] puts a bound on an operator scaling as g_S/M_S^2 where he takes g_S to be $g_{YM}^2 = 0.4$. With this assumption the string scale is higher than about 3 TeV.

However, this bound assumes a particular model and a particular string coupling. It could readily change by order unity if either of these assumptions is abandoned. Furthermore, we don't know if quark lepton operators are generated with the same or comparable coefficients.

It should be noted that if we take weak string coupling to avoid the bound, we don't improve the viability of black hole searches since black holes would form at M_S/g_s^2 whereas string balls would form at a scale M_S/g_S.

References

[1] N. Arkani-Hamed, S. Dimopoulos and G. R. Dvali, Phys. Lett. B **429**, 263 (1998) [arXiv:hep-ph/9803315]. I. Antoniadis, N. Arkani-Hamed, S. Dimopoulos and G. R. Dvali, Phys. Lett. B **436**, 257 (1998) [arXiv:hep-ph/9804398]. L. Randall and R. Sundrum, Phys. Rev. Lett. **83**, 3370 (1999) [arXiv:hep-ph/9905221]. L. Randall and R. Sundrum, Phys. Rev. Lett. **83**, 4690 (1999) [arXiv:hep-th/9906064].

[2] S. Dimopoulos and G. L. Landsberg, Phys. Rev. Lett. **87**, 161602 (2001) [arXiv:hep-ph/0106295].

[3] S. B. Giddings and S. D. Thomas, Phys. Rev. D **65**, 056010 (2002) [arXiv:hep-ph/0106219].

[4] P. C. Argyres, S. Dimopoulos and J. March-Russell, Phys. Lett. B **441**, 96 (1998) [arXiv:hep-th/9808138].

[5] T. Banks and W. Fischler, arXiv:hep-th/9906038.

[6] S. W. Hawking, Commun. Math. Phys. **43**, 199 (1975) [Erratum-ibid. **46**, 206 (1976)].

[7] J. L. Hewett, Phys. Rev. Lett. **82**, 4765 (1999) [arXiv:hep-ph/9811356].

[8] G. F. Giudice and A. Strumia, Nucl. Phys. B **663**, 377 (2003) [arXiv:hep-ph/0301232].

[9] P. Burikham, T. Han, F. Hussain and D. W. McKay, Phys. Rev. D **69**, 095001 (2004) [arXiv:hep-ph/0309132].

[10] S. Cullen, M. Perelstein and M. E. Peskin, Phys. Rev. D **62**, 055012 (2000) [arXiv:hep-ph/0001166].

[11] I. Antoniadis, K. Benakli and A. Laugier, JHEP **0105**, 044 (2001) [arXiv:hep-th/0011281].

[12] Greg Landsberg , "Randall Sundrum Black Holes at the LHC", DPF 2006. G. L. Landsberg, J. Phys. G **32**, R337 (2006) [arXiv:hep-ph/0607297].

[13] L. A. Anchordoqui, H. Goldberg and A. D. Shapere, Phys. Rev. D **66**, 024033 (2002) [arXiv:hep-ph/0204228].

[14] J. M. Campbell, J. W. Huston and W. J. Stirling, Rept. Prog. Phys. **70**, 89 (2007) [arXiv:hep-ph/0611148].

[15] R. C. Myers and M. J. Perry, Annals Phys. **172**, 304 (1986).

[16] W. M. Yao *et al.* [Particle Data Group], J. Phys. G **33**, 1 (2006).

[17] G. F. Giudice, R. Rattazzi and J. D. Wells, Nucl. Phys. B **544**, 3 (1999) [arXiv:hep-ph/9811291].

[18] L. A. Anchordoqui, J. L. Feng, H. Goldberg and A. D. Shapere, Phys. Lett. B **594**, 363 (2004) [arXiv:hep-ph/0311365].

[19] R. Emparan, G. T. Horowitz and R. C. Myers, Phys. Rev. Lett. **85**, 499 (2000) [arXiv:hep-th/0003118].

[20] M. Cavaglia, Phys. Lett. B **569**, 7 (2003) [arXiv:hep-ph/0305256].

[21] J. Preskill, P. Schwarz, A. D. Shapere, S. Trivedi and F. Wilczek, Mod. Phys. Lett. A **6**, 2353 (1991).

[22] P. D. D'Eath and P. N. Payne, Phys. Rev. D **46**, 658 (1992).

[23] P. D. D'Eath and P. N. Payne, Phys. Rev. D **46**, 675 (1992).

[24] D. M. Eardley and S. B. Giddings, Phys. Rev. D **66**, 044011 (2002) [arXiv:gr-qc/0201034].

[25] H. Yoshino and Y. Nambu, Phys. Rev. D **67**, 024009 (2003) [arXiv:gr-qc/0209003].

[26] H. Yoshino and V. S. Rychkov, Phys. Rev. D **71**, 104028 (2005) [arXiv:hep-th/0503171].

[27] J. D. Bekenstein and V. F. Mukhanov, Phys. Lett. B **360**, 7 (1995) [arXiv:gr-qc/9505012].

[28] G. T. Horowitz and J. Polchinski, Phys. Rev. D **55**, 6189 (1997) [arXiv:hep-th/9612146].

[29] B. Abbott *et al.* [D0 Collaboration], Phys. Rev. Lett. **82**, 2457 (1999) [arXiv:hep-ex/9807014].

[30] S. Esen, R. Harris, "CMS Sensitivity to Quark Contact Interactions using Dijets" CMS-NOTE-2006-071.

[31] M. Cavaglia, R. Godang, L. Cremaldi and D. Summers, arXiv:hep-ph/0609001. M. Cavaglia, R. Godang, L. M. Cremaldi and D. J. Summers, JHEP **0706**, 055 (2007) [arXiv:0707.0317 [hep-ph]].

[32] C. M. Harris, P. Richardson and B. R. Webber, JHEP **0308**, 033 (2003) [arXiv:hep-ph/0307305].

[33] G. Landsberg, TrueNoir Monte Carlo, http://hep.brown.edu/users/Greg/TrueNoir/

[34] L. Susskind, arXiv:hep-th/9501106.

[35] D. J. Gross and P. F. Mende, Nucl. Phys. B **303**, 407 (1988). D. J. Gross and P. F. Mende, Phys. Lett. B **197**, 129 (1987).

[36] S. Dimopoulos and R. Emparan, Phys. Lett. B **526**, 393 (2002) [arXiv:hep-ph/0108060].

[37] P. Horava, Phys. Rev. D **59**, 046004 (1999) [arXiv:hep-th/9712130].

[38] D. Bourilkov, "Compositeness search with dimuons in CMS" CMS-NOTE-2006-085.

[39] J. Polchinski and M. J. Strassler, Phys. Rev. Lett. **88**, 031601 (2002) [arXiv:hep-th/0109174].

[40] M. R. Douglas, D. Kabat, P. Pouliot and S. H. Shenker, Nucl. Phys. B **485**, 85 (1997) [arXiv:hep-th/9608024].

[41] I. Bars and I. Hinchliffe, Phys. Rev. D **33**, 704 (1986).

[42] E. Eichten, K. D. Lane and M. E. Peskin, Phys. Rev. Lett. **50**, 811 (1983).

[43] K. D. Lane, arXiv:hep-ph/9605257.

[44] V. M. Abazov *et al.* [D0 Collaboration], Phys. Rev. Lett. **95**, 091801 (2005) [arXiv:hep-ex/0505018].

[45] N. Arkani-Hamed, M. Porrati and L. Randall, JHEP **0108**, 017 (2001) [arXiv:hep-th/0012148].

[46] S. B. Giddings, Phys. Rev. D **67**, 126001 (2003) [arXiv:hep-th/0203004].

[47] R. Contino, L. Pilo, R. Rattazzi and A. Strumia, JHEP **0106**, 005 (2001) [arXiv:hep-ph/0103104].

[48] T. G. Rizzo, Phys. Lett. B **647**, 43 (2007) [arXiv:hep-ph/0611224].

[49] P. Burikham, T. Figy and T. Han, Phys. Rev. D **71**, 016005 (2005) [Erratum-ibid. D **71**, 019905 (2005)] [arXiv:hep-ph/0411094].

[50] R. Emparan, G. T. Horowitz and R. C. Myers, JHEP **0001**, 007 (2000) [arXiv:hep-th/9911043]. S. B. Giddings, E. Katz and L. Randall, JHEP **0003**, 023 (2000) [arXiv:hep-th/0002091]. S. B. Giddings and E. Katz, J. Math. Phys. **42**, 3082 (2001) [arXiv:hep-th/0009176]. R. Emparan, A. Fabbri and N. Kaloper, JHEP **0208**, 043 (2002) [arXiv:hep-th/0206155].

[51] G. F. Giudice, R. Rattazzi and J. D. Wells, Nucl. Phys. B **630**, 293 (2002) [arXiv:hep-ph/0112161].